CHALMERS
UNIVERSITY OF TECHNOLOGY

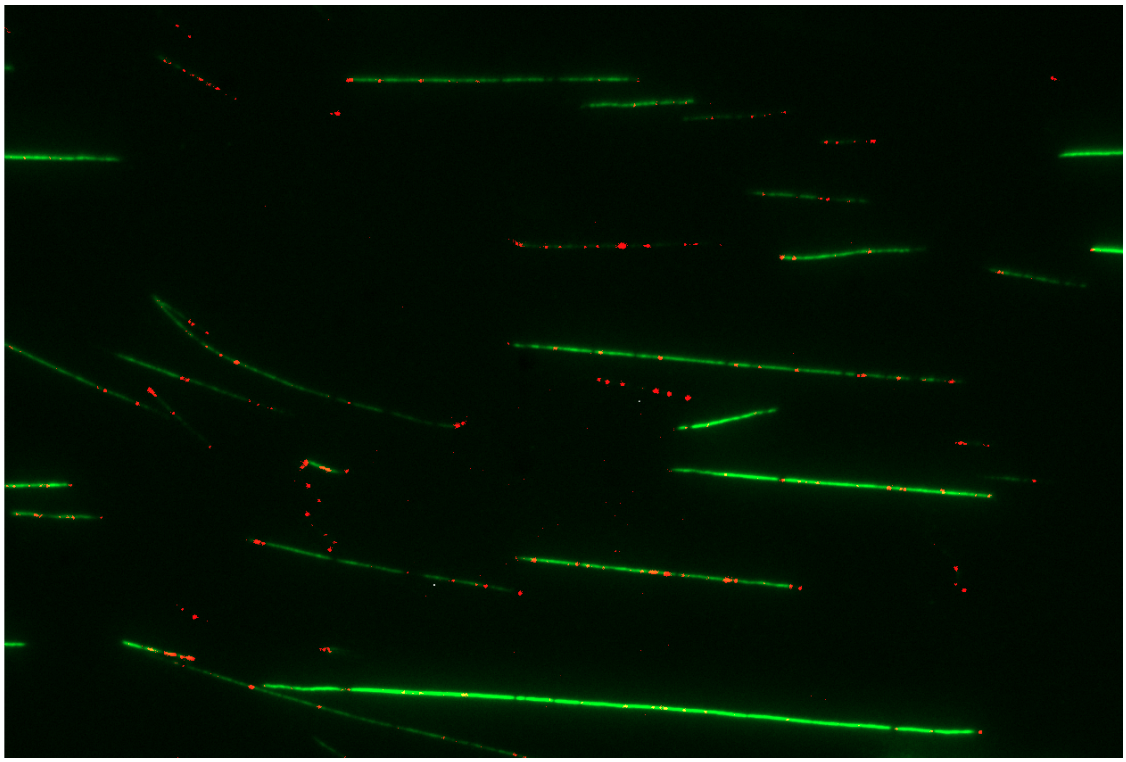

Single Molecule Imaging for Detecting DNA Damage in Bacteria

Master's thesis in Biotechnology

JOHANNA CARLSON

DEPARTMENT OF LIFE SCIENCES

CHALMERS UNIVERSITY OF TECHNOLOGY
Gothenburg, Sweden 2023
www.chalmers.se

Master's thesis 2023

Single Molecule Imaging for Detecting DNA Damage in Bacteria

JOHANNA CARLSON

CHALMERS
UNIVERSITY OF TECHNOLOGY

Department of Life Sciences
Division of Chemical Biology
Wenzel Research Group & Westerlund Research Group
Chalmers University of Technology
Gothenburg, Sweden 2023

Single Molecule Imaging for Detecting DNA damage in Bacteria
JOHANNA CARLSON

Supervisor: Margareth Sidarta, Michaela Wenzel and Obed Aning, Department of Life Sciences
Examiner: Michaela Wenzel, Department of Life Sciences

Master's Thesis 2023
Department of Life Sciences
Division of Chemical Biology
Westerlund Research Group & Wenzel Research Group
Chalmers University of Technology
SE-412 96 Gothenburg
Telephone +46 31 772 1000

Cover: Stretched bacterial DNA stained with YOYO-1 with damaged parts in red, visualized with fluorescence microscopy.

Typeset in LaTeX
Printed by Chalmers Reproservice
Gothenburg, Sweden 2023

Single Molecule Imaging for Detecting DNA Damage in Bacteria
JOHANNA CARLSON
Department of Life Sciences
Chalmers University of Technology

Abstract

As antibiotic resistance increases, there is a growing interest in developing new strategies and targets for antibiotics to combat this issue. However, the mechanisms of action for antibiotics, particularly their effect on bacterial DNA, are often not fully understood. This lack of knowledge can hinder the application of DNA damaging agents as antibiotics. In this project, a fluorescence microscopy-based method was developed to analyze bacterial DNA damage caused by stressors such as chemicals and antibiotics. The method relied on enzymes that are part of the base excision repair system for single-strand DNA damage. These enzymes were responsible for removing different types of damage. To visualize the DNA damage, fluorescently labeled nucleotides were incorporated and observed using fluorescence microscopy. This method had not been previously employed to analyze DNA damage in bacteria. During the optimization process, several factors were identified as crucial for ensuring DNA quality and detecting DNA damage. The purity of chemicals used and the quantity of DNA were observed to be important. Additionally, it was discovered that the act of repeated temperature shock of *B. subtilis* potentially caused DNA damage. Although progress has been made, further studies are required to develop a more reproducible and robust method for detecting DNA damage caused by different antibiotics.

Keywords: antibiotics, DNA damage, single molecule imaging, bacillus subtilis, fluorescence microscopy, base excision repair.

Acknowledgements

I want to thank Fredrik Westerlund and Michaela Wenzel for the opportunity to perform this project. I want to thank Michaela for all guidance and support during my project. I want to thank my supervisors Margareth Sidarta and Obed Aning for the help with the experimental work and for all support and advice. It would not have been possible without you. I would also like to thank all members of the Wenzel and Westerlund groups that have contributed to a nice work environment. Lastly, I want to thank my family and friends for their support throughout my studies.

Johanna Carlson, Gothenburg, June 2023

List of Acronyms

Below is the list of acronyms that have been used throughout this thesis listed in alphabetical order:

AP	Apurinic/Apyrimidinic
APE1	AP endonuclease 1
APTES	3-Aminopropyl-triethoxysilane
ATMS	Allyltrimethoxysilane
BCP	Bacterial Cytological Profiling
BER	Base Excision Repair
Cipro	Ciprofloxacin
DAPI	4,6-diamidino-2-phenylindole
DSB	Double-strand break
dsDNA	Double-stranded DNA
EDTA	Ethylenediaminetetraacetic acid
Endo III	Endonuclease III
Endo IV	Endonuclease IV
Endo VIII	Endonuclease VIII
Fpg	DNA-formamidopyrimidine glycosylase
LB	Luria-Bertani
MOA	Mechanism Of Action
NER	Nucleotide Excision Repair
NFT	Nitrofurantoin
ROS	Reactive oxygen species
SMI	Single molecule imaging
SSB	Single-strand break
ssDNA	Single-stranded DNA
TBE	Tris-borate EDTA
Tet	Tetracycline
Trim	Trimethoprim
UDG	Uracil DNA glycosylase

Contents

List of Figures

List of Tables

1
Introduction

The discovery of antibiotics has made treatment of previously deadly bacterial infection diseases become possible. Antibiotics also have important applications in surgeries, organ transplantations and have been exploited for use as chemotherapeutic agents [3]. However, the recent decline in newly discovered antibiotics parallel to an increase of resistance against the existing ones, has led to less efficient and successful treatments for patients [3, 4]. Antibiotic resistance is, according to the World Health Organization, one of humanity's biggest global health problems [4]. Some of the main causes of antibiotic resistance include overuse and misuse in human health and animal industry, poor sanitation and sewage system and wildlife spread [4, 5].

As antibiotic resistance is a global problem, it is important to develop new strategies or new targets for antibiotics. There are different ways antibiotics target bacteria; cell wall synthesis, cell membrane, protein synthesis, nucleic acid synthesis, and bacterial metabolic pathways [6]. Despite of already known targets, many of their exact mechanisms of action (MOA) and how they affect and act against bacteria are not completely understood, especially for the effect on bacterial DNA. Thus, it hinders the application of DNA damaging agents as antibiotics.

DNA damage can occur through various mechanisms, including oxidative damage, alkylation of bases, base loss, formation of bulky adducts, DNA crosslinking and DNA strand breaks [7]. Single-strand DNA (ssDNA) damage is a frequent occurrence and can be induced by external stressors like UV or certain drug molecules. Bacteria possess repair pathways that are activated in response to DNA damage, and the primary pathway involved in repairing ssDNA damage is the base excision repair (BER) pathway.

DNA damaging effects caused by antibiotics have for example been evaluated using the comet assay, to investigate single-stand breaks (SSB) and double-strand breaks (DSB)[8]. Other methods include measuring the SOS response, that activate DNA repair pathways [9] and the utilization of biomarkers to recognize specific types of DNA damage [10]. Common for many methods is that they either address one specific damage type, alternatively only provide a qualitative assessment whether DNA damage is present or not, lacking specificity.

Zirkin *et al.* developed a single molecule imaging (SMI) approach to detect multiple types of ssDNA damage simultaneously. The method utilizes enzymes that are part of the BER system that can identify different types of damages and remove those bases [1], see Figure 1.1. This leaves a gap where fluorescently labelled nucleotides can be incorporated with DNA polymerase. The DNA backbone is in addition stained with YOYO-1 and visualized with a fluorescence microscope. The

DNA damage is quantified by measuring the length and the number of damaged sites on the DNA. Using hydrogen peroxide as ROS inducer, they showed that hydrogen peroxide concentration is directly proportional with the DNA damage level, indicating that the method is able to distinguish and compare damage with high sensitivity. Until now, this been used in various applications, such as to quantify DNA damage induced by bleomycin, a chemotherapy drug or by topoisomerase II poison etoposide [11, 12]. However, it has not yet been used to analyze the DNA damage in bacteria caused by antibiotics.

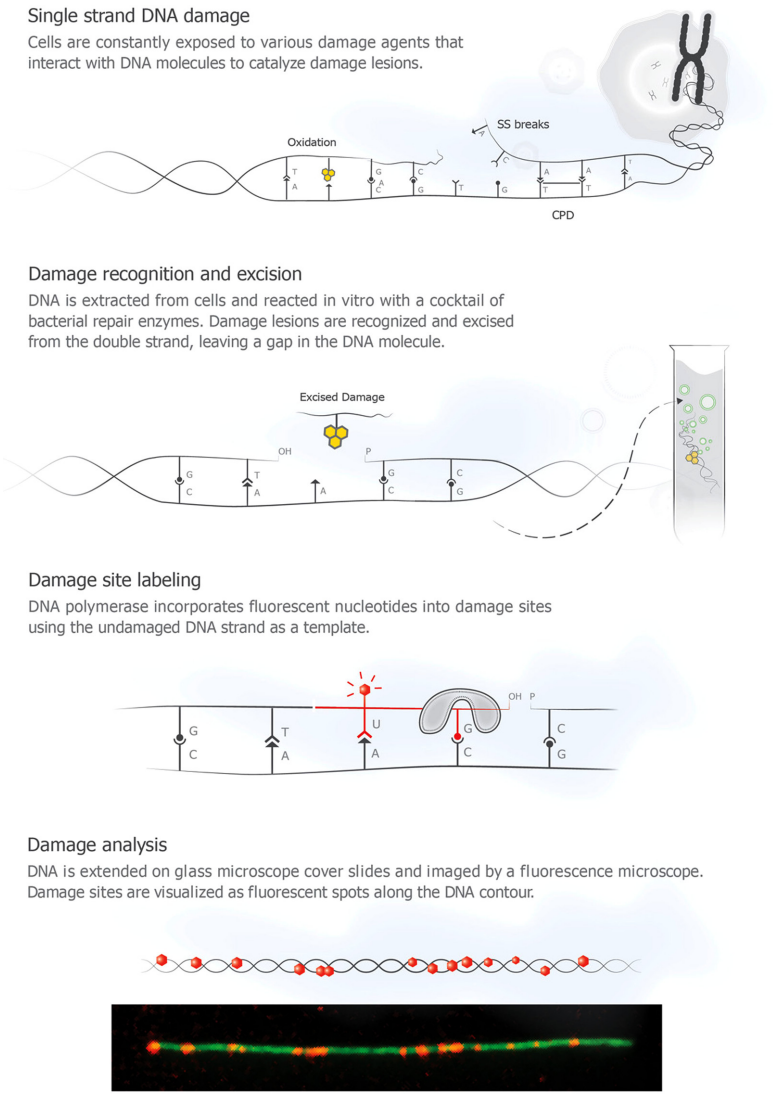

Figure 1.1: Single molecule imaging approach to detect DNA damage. DNA is exposed to DNA damaging agents. Bacterial repair enzymes recognize and remove single-stranded DNA damage, leaving gaps where fluorescently labeled nucleotides are incorporated. The DNA is then stretched and imaged with fluorescence microscopy. Reprinted with permission from [1]. Copyright 2023 American Chemical Society.

1.1 Aim

The aim of project is to develop a fluorescence microscopy-based method to analyze bacterial DNA damage caused by various stressors, such as chemicals or different antibiotics.

1.2 Limitations

In this study, Gram-positive bacteria *Bacillus subtilis* was used as the model organism. Due to time limitation, there were no experiments conducted using any Gram-negative bacteria such as *Escherichia coli* or other model organisms. Besides, this work was more focused on the optimization and proof of concept of the method. Some initial experiments using antibiotics had been conducted in this work. However, further experiments using additional antibiotics will be needed in the future.

2
Theory

The theory is divided into part that describes the model organism, DNA damage and repair, and some of the methods utilized in the study.

2.1 *Bacillus subtilis*

B. subtilis is a rod-shaped Gram-positive bacterium that has a generation time of approximately 20 minutes in the optimal temperature span of 30-37℃[13]. It is widely used as a model organism and characterized as a Generally Considered As Safe (GRAS) organism. It can form endospores due to nutritional starvation and other stress in the environment. As other bacteria, it has circular chromosomal DNA that resides in a super-coiled formation in the nucleoid, making it easy to extract and study the DNA [14].

2.2 DNA damage

DNA is found in every known organism and encodes for essential information responsible for the overall function of the organism [15]. DNA is a double-helical structure composed of two strands. These strands are made up of a sugar-phosphate backbone connected to multiple nitrogenous bases through glycosidic bonds. A nitrogenous base is either a pyrimidine; thymine (T) or cytosine (C), or a purine; adenine (A) or guanine (G). In the double helix, A binds to T and C binds to G through hydrogen bonds. During transcription, the DNA strands are used as a template and the corresponding bases are added, except for T that is substituted by uracil (U), to create RNA.

DNA can be damaged in different ways, including base damage sites in which the damage is small or bulky, apurinic/apyrimidinic (AP) sites, single or double stranded breaks, cross-links, ribonucleotide misincorporation and base-pair mismatch [7] . DNA damage is either of endogenous or exogenous source. Endogenous source is the reactive byproducts formed during normal cellular metabolism [16]. A common source of endogenous damage are reactive oxygen and nitrogen species [7]. Exogenous source are environmental, physical, and chemical agents and factors. Common sources are UV or chemicals such as antibiotics and may affect the DNA directly or indirectly. Damaging DNA can affect the fitness and viability of the bacterium, thus making it a good target for antibiotics.

2.3 DNA repair

There are different pathways for DNA repair that are activated when the DNA is damaged in *B. subtilis* [16]. Some examples of that are the SOS response (Figure 2.1) that activates repair pathways, the nucleotide excision repair (NER) (Figure 2.2) and the base excision repair (BER) (Figure 2.3). Which one of the pathways that is activated depends mostly on the type of DNA damage.

2.3.1 SOS response

The SOS response system (Figure 2.1) is activated in response to DNA damage caused by endo- and exogenous sources [17]. It is very well known and characterized for *E. coli* and has been shown to work similarly in *B. subtilis* [16]. It is a response in which DNA repair and mutagenesis are activated while the cell cycle is stopped [18]. LexA acts as a transcriptional repressor, while RecA activates the response. When the DNA is damaged and goes through replication, ssDNA is formed, to which the RecA can bind. When bound it turns into its active form and activates LexA that self-cleaves and derepresses over 50 genes under its control.

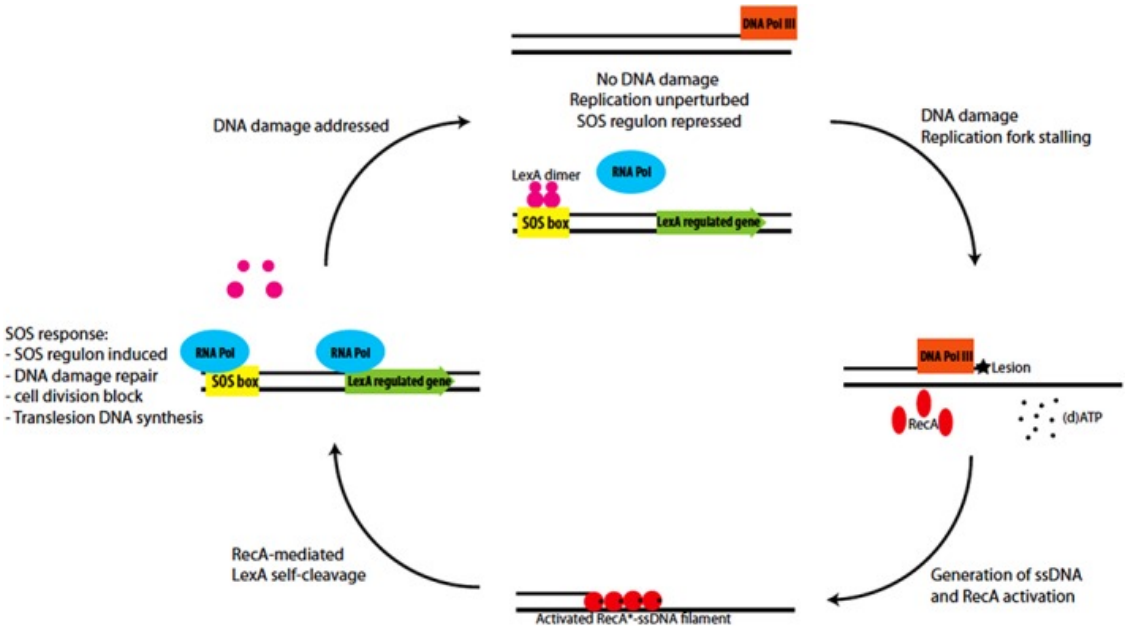

Figure 2.1: Schematic of the SOS response. When the replication is stalled at the damaged site ssDNA is formed and RecA can bind to it and turn its active form. LexA self-cleaves and that causes derepression of genes and the DNA damage can be addressed. Reused with permission from [2].

2.3.2 Nucleotide excision repair (NER)

The NER pathway (Figure 2.2) repairs different types of lesions, often bulky lesions such as damage induced by UV or drugs [16]. The repair pathway is controlled by the Uvr system, which includes UvrA, UvrB and UvrC. The SOS response regulates the

uvrBA genes, while the *uvrC* gene is located on another position. Damaged bases are identified by a complex of UvrA and UvrB. When the damage is recognized, UvrA dissociates from the complex and UvrC is recruited to the site by UvrB. They then remove 10-15 nucleotides around the non-coding base, which is then removed by DNA helicase II (UvrD). The resulting gap is filled with DNA polymerase I and finally sealed by DNA ligase.

A subpathway that exists within NER is called transcription-coupled repair (TCR), in which the mutation frequency decline (Mfd) protein is involved [16]. When RNA polymerase is stalled at a damaged site, the Mfd protein dislodges it and initiates repair on the transcribed strand.

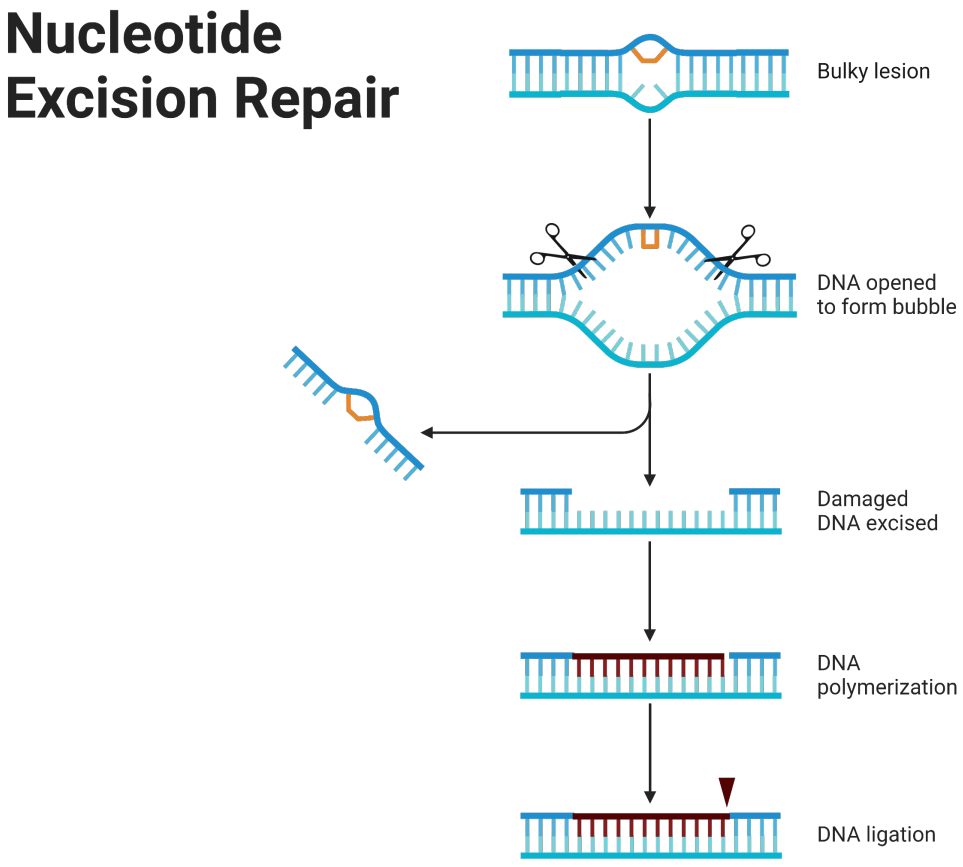

Figure 2.2: Simplified schematic of the Nucleotide Excision Repair (NER) pathways. A bulky lesion is recognized and the DNA is opened up. The damaged part and nucleotides around are excised, and new nucleotides are incorporated. Created in Biorender.com.

2.3.3 Base excision repair (BER)

In contrast to NER, the BER pathway (Figure 2.3) repairs non-bulky DNA damage caused by, for example, alkylation, oxidation, depurination/depyrimidination,

deamination, and dUTP incorporation [16]. BER is the DNA repair pathway that is the most frequently used. Damaged nitrogenous bases are recognized by glycosylases, a family of enzymes. Monofunctional glycosylases remove the damaged base by hydrolyzing the N-glycosidic bond and thus creating a Apurinic/apyrimidinic (AP) site, in which the sugar-phosphate backbone is still intact [7]. The AP site is then recognized by enzymes that nick the 3' and 5' end of the site, allowing for DNA polymerase I to incorporate nucleotides. Bifunctional glycosylases remove the damaged base and cleave the phosphodiester backbone through β-elimination, making it possible to incorporate new nucleotides.

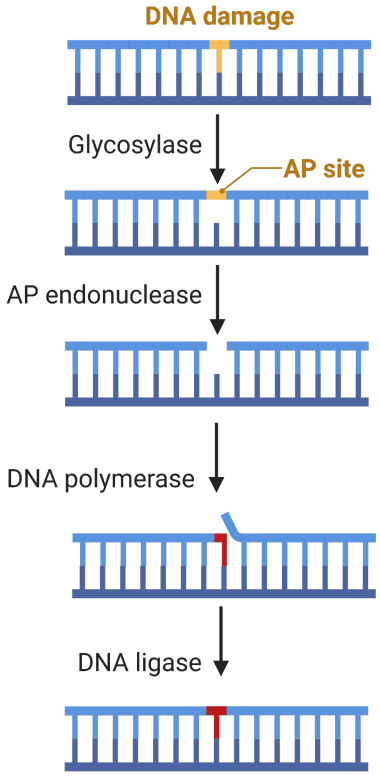

Figure 2.3: Simplified schematic of the Base Excision Repair (BER). Glycosylase recognizes and removes a damage base, creating an AP-site. An AP endonuclease nicks the backbone and creates a gap where nucleotides are incorporated. Created in Biorender.com.

There is a system that specifically repairs oxidized guanines, such as 8-oxoguanine. That kind of damage is removed by the glycosylase Fpg [7, 16]. It is the most commonly occurring type of oxidative damage and if not removed it is very mutagenic. Another type of damage is when uracil is incorporated in double-stranded DNA (dsDNA). This is possible when dUMP is incorporated instead of dTMP or as a result of deamination of dCMP to dUMP. It can occur either spontaneously or as a result of exposure to DNA damaging agents. To remove the damage, BER and the specific glycosylase UDG is activated. AP sites can occur both during BER as well as spontaneously and are recognized and repaired by AP endonucleases.

The mixture of BER enzymes that are used in the project were chosen based on previous papers [1, 11, 12], and are summarized with a short description of functions in Table 2.1. The enzymes repair various types of damage in the DNA, mostly different types of oxidative damage.

Table 2.1: Enzymes that are used in the project and their functions.

Enzyme	Function
APE1	Repairs apurinic/apyrimidinic (AP)-sites [19]. Recognizes and removes uracil, alkylated and oxidized bases and AP-sites [20].
FPG	Recognizes and removes various types of oxidized purines, for example 8-oxoguanine[1].
Endo III	Can remove oxidized pyrimidines [21].
Endo IV	Apurinic/apyrimidinic (AP) endonuclease, repairs oxidative DNA damage [1].
Endo VIII	Repairs various types of damaged pyrimidines, including oxidized pyrimidines [1].
UDG	Catalyzes the removal of uracil from DNA, such as those caused by deamination of cytosine to uracil [1].

2.4 Antibiotics

The antibiotics that were chosen in the project were picked mostly based on previous findings in the Wenzel research group (Chalmers University of Technology) that suggested impact on DNA. The antibiotics as well as the corresponding targets and the previously known MOA:s can be seen in Table 2.2. Most of the antibiotics have MOA:s that are not fully understood or may have multiple targets in bacteria.

Table 2.2: The antibiotics used in the project and their targets and known mechanisms of action.

Antibiotic	Targets	Mechanism of action
Nitrofurantoin	Cellular macromolecules	It forms an unknown reactive species, likely containing nitrogen, leading to damage to DNA, proteins and lipids [22, 23].
Ciprofloxacin	DNA gyrase, topoisomerase IV	Binds to DNA gyrase and topoisomerase IV, inhibiting DNA synthesis and introducing DNA double stranded break (DSBs) DNA [24].
Tetracycline	Protein synthesis	Prevents aminoacyl-tRNA from attaching to the ribosomal acceptor site and thus inhibits protein synthesis [25].
Trimethoprim	Folic acid pathway	Inhibits the enzyme dihydrofolate reductase which blocks the reduction of dihydrofolate to tetrahydrofolate. The inhibition of the tetrahydrofolate production affects the DNA replication and protein synthesis [26].
Mitomycin C	DNA synthesis	It inhibits DNA synthesis by crosslinking complementary strands of the DNA [27].
Zeocin	DNA	Induces double-stranded-breaks in the DNA by intercalating into the DNA [28].
Echinomycin	DNA	Binds to double-helical DNA by intercalating [29, 30]. As a result of that, the thermal stability of the double-stranded DNA increases with no single- or double-stranded breaks [30].

2.5 Bacterial Cytological Profiling (BCP)

Bacterial Cytological Profiling (BCP) is a fluorescence light microscopy-based method, first described in 2013, that can be used to visualize different cellular components [31, 32]. It is used with different kind of dyes that visualized different parts of the bacterium. The dye 4,6-diamidino-2-phenylindole (DAPI) is used to stain DNA, while the dye Nile red is commonly used to stain the cell membrane, in addition a fluorescent fusion protein of interest can be used. BCP is a quick and simple method and can to investigate the cellular pathways that are targeted by a specific compound of interest.

2.6 Single Molecule Imaging (SMI)

SMI, in comparison to BCP, is a method in which single molecules are visualized and analyzed and the heterogeneity of a sample is taken into consideration [33]. In this project SMI refers to the method of visualizing single DNA molecules with fluorescence microscopy and then analyzing the damage on the individual DNA molecules. To be able to analyze the damage and the length, the DNA molecules need to be stretched out, as they normally exist in a coiled state in bacteria. This can be achieved in different ways and one example is to use glass slides and glass coverslips that have been functionalized, for example by using a mixture of Allyltrimethoxysaline (ATMS) and (3-Aminopropyl) trimethoxysilane mixed with acetone [34]. ATMS with its hydrophobic groups and APTES with its hydrophilic and positively charged groups makes it possible for the negatively charged DNA molecules to bind to the surface. By adding DNA sample at the edge of the coverslip on the glass slide, capillary force pulls the DNA between the glasses and stretches the DNA, see Figure 2.4. To be able to visualize the DNA it is often stained with a DNA binding dye, such as the green fluorescent dye YOYO-1. The SMI method that is used in the project uses, as mentioned, a mixture of naturally occurring BER enzymes to identify damaged parts on the DNA strands and remove them, leaving gaps in the DNA [1]. The gaps are then filled with fluorescently labeled nucleotides, the DNA stained with YOYO-1 and visualized with fluorescence microscopy. In the following thesis, the described method is referred to as the SMI method.

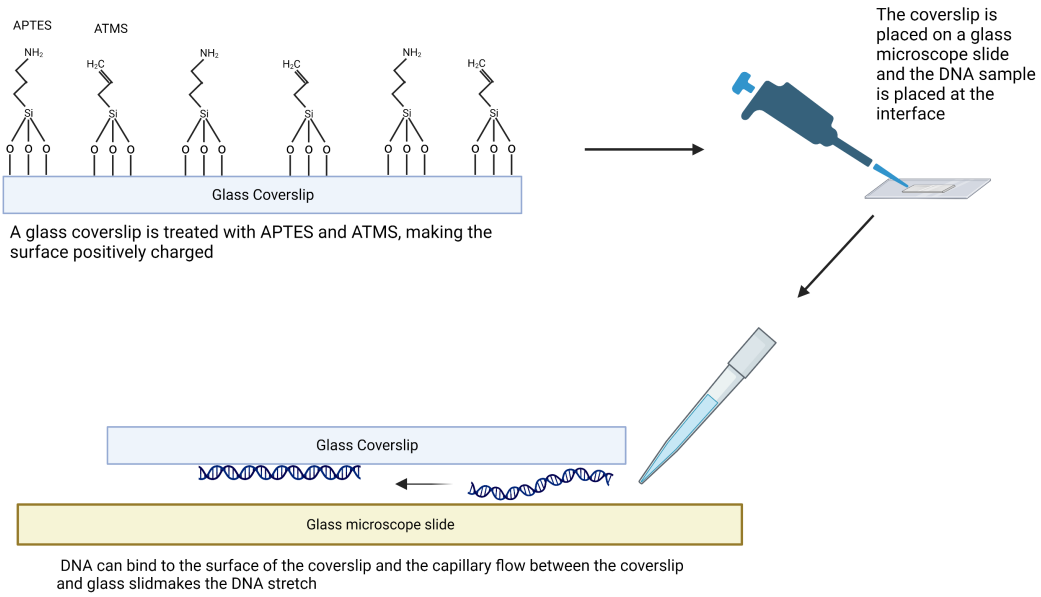

Figure 2.4: Schematic of the stretching of DNA using APTES and ATMS. The coverslip is immersed into a solution of acetone, APTES and ATMS that makes it possible for DNA to bind. When the DNA solution is put at the interface of a glass slide and a coverslip, capillary force pulls the DNA between the glasses and stretches the DNA. Created in Biorender.com.

3

Material and Methods

The method is divided into three main parts: Initial, optimizing and antibiotic experiments.

3.1 Chemicals

Table 3.1: Some of the chemicals used in the project and the manufacturer.

Chemical	Manufacturer	Remark
Ciprofloxacin	Fisher Scientific	Antibiotic
Echinomycin	Fisher Scientific	Antibiotic
Mitomycin C	Fisher Scientific	Antibiotic
Nitrofurantoin	Fisher Scientific, Acros Organic	Antibiotic
Trimethoprim	Fisher Scientific	Antibiotic
Tetracycline	Fisher Scientific	Antibiotic
Zeocin	Fisher Scientific	Antibiotic
DAPI	Fisher Scientific	DNA stain, BCP
Nile red	Fisher Scientific	Lipophilic stain, BCP
APE1	New England Biolabs (NEB)	Enzyme
Endonuclease III	New England Biolabs (NEB)	Enzyme
Endonuclease IV	New England Biolabs (NEB)	Enzyme
Endonuclease VIII	New England Biolabs (NEB)	Enzyme
FPG	New England Biolabs (NEB)	Enzyme
UDG	New England Biolabs (NEB)	Enzyme
YOYO-1	Invitrogen	DNA dye, SMI method
dATP	New England Biolabs (NEB)	Nucleotide
dCTP	New England Biolabs (NEB)	Nucleotide
dGTP	New England Biolabs (NEB)	Nucleotide
dTTP	New England Biolabs (NEB)	Nucleotide
Aminoallyl-dUTP-ATTO-647 N	Jena Bioscience	Fluorescent nucleotide
APTES	Sigma-Aldrich	SMI method
ATMS	Sigma-Aldrich	SMI method

3.2 Initial experiments

Initial experiments comprise experiments done to establish the methodology, before optimization experiments.

3.2.1 Culture preparation and treatment

List of the bacterial strains used in this work can be seen in Table 3.2. Bacterial cells were grown in 2 mL LB and incubated overnight at 37℃ while shaking. For strain UG10, cells were grown at 30℃ instead of 37℃. On the next day, cells were diluted 1:100 in 20 mL LB and grown to an OD_{600} of 0.3-0.35. After that, cells were treated with 0.3% v/v H_2O_2 for 30 minutes

Table 3.2: The strains used in the project.

Strain	Genotype[a]	Origin	Application
168CA	*trpC2*	DSMZ[b] [35]	SMI method
UG10	*trpC2 amyE::Pxyl_recA-mgfp spc*	[36]	BCP
BKE16940	*trpC2 ΔrecA::ery*	BGSC[c] [37]	SMI method (Appendix C.1)
2682	*trpC2 recA::tet*	[38]	SMI method Appendix C.1)

[a] "spc" stands for resistance against spectinomycin, "tet" stands for resistance against tetracycline, "ery" stands for resistance against erythromycin, and mgfp is a Green Fluorescent Protein
[b] The Leibniz Institute DSMZ-German Collection of Microorganisms and Cell Cultures GmbH
[c] Bacillus Genetic Stock Center (BGSC)

3.2.2 DNA Isolation

DNA isolation method is based on the standard phenol-chloroform isolation with some modifications [39]. The complete protocol can be seen in Appendix A.2. In short, samples were centrifuged, the pellet washed in TES buffer and then once again centrifuged. The pellet was resuspended in TES and incubated (37℃) with Lysozyme and RNase for 30 minutes and then with Pronase and Sarkosyl for 60 minutes. In accordance with the standard protocol an equal amount of phenol and chloroform was added, and the samples were mixed and centrifuged. The upper aqueous phase containing the DNA was transferred to a new tube, chloroform was added, the samples were mixed and finally centrifuged. The upper layer was once again transferred to a new tube and isopropanol was added and the samples were mixed and centrifuged. The DNA pellet was washed twice in ethanol 70%, dried, and finally solubilized in milli-Q water.

The concentration of the DNA was, during the initial experiments, measured with two different methods, NanoDrop^{TM} (ND-1000 UV-Vis Spectrophotometer, Thermo Fisher) and Qubit 4 Fluorometer (Invitrogen, Thermo Fisher, USA) with dsDNA

Broad Range Assay kit. The measurements were carried out according to the respective manufacturer protocols.

DNA was stored in -20℃ or -80℃ (longer storage). At all times when DNA in solution was handled, either a cut pipette tip or a wide bore pipette tip was used to minimize breakage of DNA.

3.2.3 SMI Method

The SMI method is based on the one previously described [1]. Briefly, an enzyme master mix (Table 3.3) was prepared in 1X CutSmart Buffer, 100 ng DNA and milli-Q water to a total volume of 50 µL per sample. Alternatively, single enzymes were added to 100 ng DNA, 1X CutSmart Buffer, and milli-Q water. The mixture was incubated (37℃) for 1 hour. A nucleotide master mix (Table 3.4) was prepared in 1.25 U DNA polymerase 1, 1X NEBuffer 2 and milli-Q water to a total volume 100 µL per sample. It was incubated (20℃) for 1 hour before the addition of 0.25 M Ethylenediaminetetraacetic acid (EDTA) to stop the ongoing reaction. During and after addition of the fluorescently labeled nucleotides, the experiments were performed in minimum light exposure. The samples were stored in -20℃ wrapped in aluminium foil.

Table 3.3: The enzymes used for DNA damage labeling and the corresponding concentration.

Enzyme	Concentration (U)
APE1	2.5
Fpg	2.5
Endo III	2.5
Endo IV	2.5
Endo VIII	2.5
UDG	2.5

Table 3.4: The nucleotides used for DNA damage labeling and the corresponding concentration.

Nucleotide	Concentration (μM)
dATP	1
dGTP	1
dCTP	1
dTTP	0.25
Aminoallyl-dUTP-ATTO-647 N	0.25

For staining and imaging, typically 7 µL of fluorescently labeled DNA was diluted in 0.5X Tris-borate EDTA (TBE) and stained with 320 nM YOYO-1. In addition, 1 µL β-mercaptoethanol was added just before the image acquisition to reduce photobleaching. From the final volume of 50 µL, 3.2 µL was placed at the interface

of a functionalized coverslip and a microscope glass slide. A drop of immersion oil was put on the coverslip and the imaging was performed with a 100X objective on a Zeiss Observer Z1 fluorescence microscope with a Photometrics Prime 95B sCMOS 22mm camera. Two channels were used for imaging, YOYO-1 (emission wavelength 508 nm) and ATTO-647 (emission wavelength 679 nm). The light source intensity was set to 20% and the exposure times were set to 370 ms and 1500 ms for YOYO-1 and ATTO-647, respectively.

Before imaging, the coverslips had to be functionalized to allow stretching of the DNA. Coverslips (22x22 mm) were arranged in a rack and immersed in a mixture of 1% v/v of 3-Aminopropyltriethoxysilane (APTES) and Allyltrimethoxysilane (ATMS) in acetone for at least 2 hours. Prior to use, they were rinsed in a solution containing acetone and milli-Q water (2:1) and dried with nitrogen gas.

3.3 Optimization Experiments

For the optimization experiments, the only difference compared to the initial experiments was the cell preparation and treatment. For DNA isolation and SMI method, see Section 3.2.2 and 3.2.3.

3.3.1 Cell Preparation and Treatment

To prepare the cell culture, a method utilizing single-use bacterial aliquots (Appendix A.1) was employed. Instead of overnight cultures, one tube of a single-use aliquot was thawed and added to 20 mL LB on the day of the DNA isolation. The cells were incubated (37℃) until an OD_{600} of 0.3-0.35 was reached. For proof-of-concept H_2O_2 with different conditions was added, see Table 3.5.

Table 3.5: Concentrations and duration times for H_2O_2 during optimization experiments.

Treatment	Stock Concentration (v/v)	Final Concentration (v/v)	Time
H_2O_2	30%	0.15%	10/30 minutes
H_2O_2	30%	0.3%	10/30 minutes

3.4 Antibiotic experiments

Some experiments with antibiotics were performed during initial and optimization experiments before the final optimization. The conditions and experiments described in Appendix C.1, in which concentrations used were based on Minimum Inhibitory Concentration (MIC) experiments and Growth Curves (GC), an example shown in Appendix D.1 and D.2.

3.4.1 Bacterial Cytological Profiling

Cells were grown overnight in 2 mL LB supplemented with 0.1% (w/v) xylose at 30 ℃ while shaking. The overnight cells were then diluted 1:100 and grown to an OD_{600} of 0.3-0.35. 100 µL of the culture was moved to pre-warmed tubes (30℃) and treated with a compound of interest, according to Table 3.6. Approximately 5 minutes before the incubation was complete, the membrane dye Nile red (0.5 µg/mL) and the DNA dye DAPI (1 µg/mL) were added to the cells. On an agarose-coated slide (1.2%), 0.5 µL of the sample was added and covered with a dopamine coated glass coverslip. The imaging was performed for no longer than 10 minutes to prevent oxygen depletion under the slide, on a fluorescence microscope (Nikon Eclipse Ti2). The images were captured in four channels: DAPI, GFP, mcCherry, and Phase. The microscope was equipped with an Okolab incubator with dark panels. The camera used was the Photometrics PRIME BSI, the objective was the CFI Plan Apochromat DM Lambda (100X Oil, N.A 1.45, W.D. 0.13 mm, Ph3) and the light source employed was the Lumencor Sola SE II FISH 365. The imaging software utilized for the microscope was Nis ELEMENTS AR 5.21.03, Nikon.

Table 3.6: The used antibiotics and their corresponding concentrations and duration times.

Antibiotic	Stock Concentration	Final Concentration	Time
Ciprofloxacin	10 mg/mL	1 µg/mL	10/30 minutes
Mitomycin C	0.5 mg/mL	0.1 µg/mL	10/30 minutes
Nitrofurantoin	10 mg/mL	25 mM	10/30 minutes
Tetracycline	10 mg/mL	2.5 µg/mL	10/30 minutes
Trimethoprim	10 mg/mL	8 µg/mL	10/30 minutes

To prepare the dopamine coated coverslips, 400 mL of a 2 mg/mL poly-L-dopamine solution was prepared by mixing 0.8 g Dopamine, 0.5 mL 0.8 M Tris-HCl (pH 8) and milli-Q water. A box of coverslips was added to the beaker and incubated for 30 minutes at room temperature. The coverslips were washed in milli-Q water and left to dry in 37℃.

3.5 Data analysis

To analyze the microscopy images acquired from the SIM method a custom-made MATLAB script was used, developed in Tobias Ambjörnsson's research group at Lund University, the settings can be seen in Appendix B.1. It worked by both recognizing DNA strands and possible Aminoallyl-dUTP-ATTO-647 N labeled dots along the strand. It calculated the total length of all recognized DNA strands and the total amount of dots and the output was presented as dots/µm. The output also contained the length of all recognized DNA molecules. The data was plotted in GraphPad 5.0.3 (for Windows, GraphPad Software, San Diego California USA, www.graphpad.com) or OriginPro, (Version 2023, OriginLab Corporation, Northampton, MA, USA).

To quantify the results from BCP, all bacteria that showed foci of RecA-GFP were counted and then divided by the total amount of bacteria in each image. The images were processed with fiji [40].

3.6 Statistics

The experiments were conducted, unless otherwise stated, in three biological replicates for each treatment condition and three technical replicates for the SMI method. Multiple images were captured for each sample to ensure statistically robust results. Statistical analysis was carried out using using GraphPad Prism 5.0.3 (for Windows, GraphPad Software, San Diego California USA, www.graphpad.com). An unpaired t-test was employed to determine if there were significant differences between the sample means. Differences were considered significant at $p<0.05$.

4
Results and Discussion

The results and discussion is divided into three parts: initial, optimization and antibiotic experiments. The data can be accessed in Appendix F.

4.1 Initial Experiments

Initial experiments were performed as a way to see whether the established SMI method used in the Westerlund group is compatible with the cell preparation method designed in the Wenzel group. This was done since the SMI method had not been applied to bacteria yet.

4.1.1 Concentration

It is important to measure the DNA concentration accurately, as the SMI method specifically requires 100 ng of DNA. If the DNA concentration is overestimated, it can be challenging to obtain images containing enough DNA strands to achieve statistically significant findings. To optimize the accuracy of DNA concentration measurement, two instruments were used: NanoDrop and the Qubit fluorometer. The DNA concentration was assessed using both NanoDrop and the Qubit fluorometer for two biological replicates, and the corresponding values are documented in Table 4.1.

Table 4.1: The measured concentration with NanoDrop and the Qubit fluorometer for DNA samples for two biological replicates.

Biological replicate	Sample	NanoDrop (ng/μL)	Qubit fluorometer (ng/μL)
1	1	755	20.6
	2	996.2	22.8
	3	697.3	21.2
2	1	565.4	28
	2	446	64.4
	3	601.7	30.6
	4	386.3	37.6

The measured concentration using NanoDrop was at all times higher than the measured concentration using the Qubit fluorometer. Although no control sample was used to confirm which instrument showed the correct measurements, it was decided

that the Qubit fluorometer would be used for the rest of the project. It has previously been shown that NanoDrop overestimates the DNA concentration and a possible explanation is that while the Qubit fluorometer specifically measures dsDNA using dyes that only fluoresce when bound to dsDNA, the NanoDrop measures all DNA (ssDNA, dsDNA, nucleotides, etc) and is more affected by impurities [41]. Therefore the Qubit fluorometer is likely more accurate for measurement of DNA concentration and more suited for this project.

4.1.2 Purity of DNA isolation Chemicals

In addition to DNA concentration, the purity of the chemicals utilized in DNA isolation are also considered crucial. For example ethanol 70%, used in the final washing step. Ethanol serves to remove salts, decrease DNA solubility, and promote DNA aggregation, if there is any contamination in the reagent, it can also contaminate the isolated DNA. Initially, a common stock of 70% ethanol was used, meaning a stock that is shared among all members in the lab. When using the common stock of ethanol several issues were observed. Firstly, the obtained microscopy images contained contaminants, affecting the recognition of DNA molecules and damaged sites in the data analysis. Secondly, the observed DNA strand did not stretch on the glass slides as expected. Lastly, it was observed that the DNA pellet became smaller and detached from the tube during ethanol washing. Upon switching to a new batch of ethanol, the mentioned issues were no longer observed (Figure E.1). New batches of isopropanol and chloroform were also prepared, to ensure that the same issues would not arise with those chemicals.

4.1.3 H_2O_2 Experiments

As a proof-of-concept, H_2O_2 was used, which can be seen in Figure 4.1. The reason H_2O_2 was chosen as the proof-of-concept is because it is a known ROS, and has previously been shown to work with the SMI method [1]. In this work, *B. subtilis* cells were treated with 0.3% H_2O_2 for of 30 minutes before isolating the DNA.

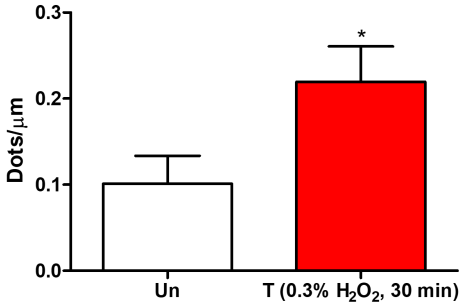

Figure 4.1: DNA damage as dots/µm for untreated (white bars) samples and for samples treated (red bars) with 0.3% H_2O_2 for of 30 minutes. Both samples are labeled with the enzyme mix (see Table 3.3). The asterisk above the treated bar denotes that the difference between the untreated and treated samples is significant ($p<0.05$). The error bars represent the standard deviation.

There was a significant difference between the means of the untreated the treated samples. This is expected since many of the enzymes recognize and remove oxidative damage. However, upon closer examination of the individual biological replicates, some variations became evident, Figure 4.2.

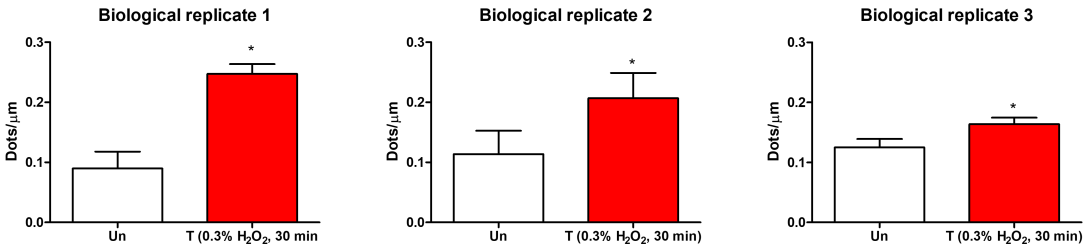

Figure 4.2: DNA damage as dots/µm for untreated (white bars) samples and for samples treated (red bars) with 0.3% H_2O_2 for 30 minutes. All samples and biological replicates were labeled with a mixture of enzymes.

A notable difference existed between the untreated sample mean and the H_2O_2 treated sample across all biological replicates. However, the significance of the difference was less pronounced in the third replicate compared to the first and second replicates, indicating of sample instability. Similar indication was visualized more clearly when the single enzyme experiment was performed, Figure 4.3. Single enzymes were used to identify the primary repair enzyme(s) involved, thereby enabling the assessment of the specific damage caused by the added compound.

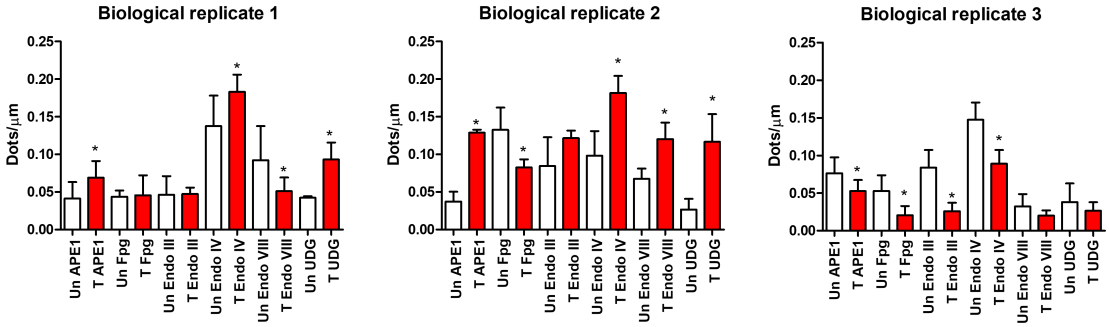

Figure 4.3: Three biological replicates visualizing DNA damage as dots/µm for untreated (white bars) and samples treated (red bars) with 0.3% H_2O_2 for 30 minutes. The DNA was labeled with a single enzyme added to each sample.

Replicate 1 and 2 generally exhibited a higher level of damage in the treated samples compared to the untreated ones, although a few exceptions were observed. However, in replicate 3, all untreated samples showed greater damage than the treated samples. The third biological DNA sample had been stored in -20℃ for approximately 2 weeks before the single enzyme experiment, possible affecting the DNA. Due to the conflicting outcomes, it was necessary to perform optimization, explained in detail in the following section.

4.2 Optimization Experiments

Optimization experiments were performed to investigate what was causing the previously mentioned issue and to provide a final optimized method that can be applied for detecting DNA damage induced by antibiotics in *B. subtilis*. The hypotheses explored were: DNA degradation during freezing and thawing, presence of contaminants, and finally bacterial stress caused by temperature shock.

The first hypothesis to explain the contradicting trend was that the DNA may have undergone degradation while stored in the freezer after DNA isolation, and then thawed for DNA damage labeling. To investigate whether this hypothesis was responsible for the damage, both DNA isolation and DNA damage labeling were performed on the same day. Both samples were treated with 0.3% H_2O_2 for 30 minutes. Based on Figure 4.4, the untreated samples displayed significant greater damage, indicating that the hypothesis linking it to the process of freezing the isolated DNA followed by thawing for SMI experiments could be ruled out.

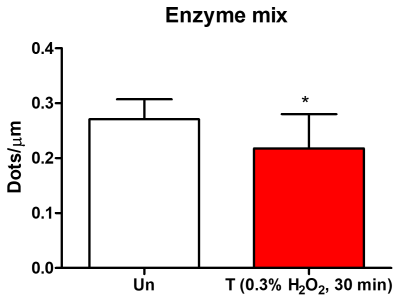

(a) Samples labeled with a mixture of enzymes.

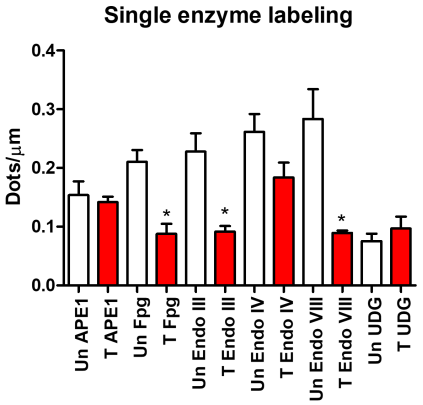

(b) Samples labeled with single enzymes.

Figure 4.4: DNA damage as dots/µm for untreated (white bars) and samples treated (red bars) with 0.3% H_2O_2 for 30 minutes. The asterisk above the bars denotes that the difference between the untreated and treated samples is significant ($p<0.05$).

An alternative hypothesis suggested that residual contaminants present in the glass Erlenmeyer flasks used during the DNA isolation procedure may have affected cellular function and induced stress, resulting in increased DNA damage. To explore this possibility, a comparison was made between: flask with normal wash (washed 1X), flask with special wash (washed 2X) and disposable plastic flask. Nevertheless, the issue remained (Figure E.2), suggesting that other factors contributed to the observed damage.

The final hypothesis was that the *B. subtilis* 168CA glycerol stock was already stressed. This hypothesis could potentially explain the increasing damage observed in the untreated samples over time (Figure 4.2 and 4.4a). A small part of the stock

may have underwent repetitive cycles of temperature shock every time it was taken out for DNA isolation and then returned to -80℃. To investigate this, a fresh stock of the strain 168CA was prepared, and the results of this investigation are presented in Figure 4.5.

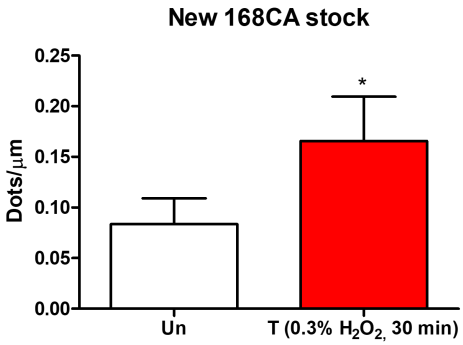

Figure 4.5: One biological replicate visualizing DNA damage as dots/µm for untreated (white bars) and samples treated (red bars) with 0.3% H_2O_2 for 30 minutes. A newly prepared stock of the *B. subtilis* strain 168CA was used. The DNA was labeled using a mixture of enzymes.

The damage of the untreated sample was much lower than previously observed and there was a significant difference between the untreated and the treated samples. This result supports the hypothesis that the damage of the untreated samples was due to stressed cells in the original stock. The reason why the untreated samples seemed more affected than the treated samples has not been established. Experiments utilizing overnight cultures were once again tried with the new stock. However, the problem with damaged untreated samples remained (Figure E.3). To prevent this from occurring again, single-use aliquots of bacteria were prepared. They were stored in -80℃ and only thawed on the day they were needed.

The final experiments were performed with the optimized method, in which single-use aliquots were used to prepare the cell cultures. The final optimization performed was regarding the treatment conditions. The bacteria seemed to be considerably more sensitive towards H_2O_2 than previously observed, the DNA molecules were very fragmented to the extent that they could not be recognized in the software. This could be since the bacteria were more healthy from the beginning and growing faster, meaning that they go through replication more and thereby are more sensitive to damage caused by H_2O_2. For that reason, a shorter treatment time, 10 minutes, and concentrations 0.15 and 0.3% were chosen, see Figure 4.6.

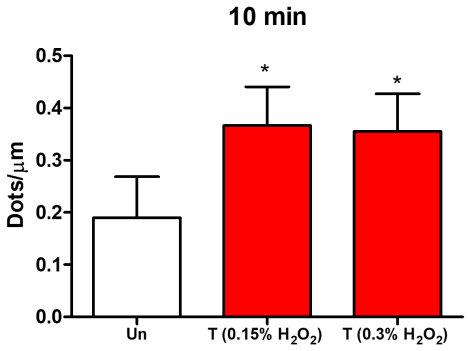

Figure 4.6: DNA damage as dots/µm for untreated (white bars) samples and for samples treated (red bars) with 0.15% and 0.3% H_2O_2 for a duration of 10 minutes. All samples are labeled with the enzyme mix.

There was a significant difference between the untreated and treated samples. Additionally, it was seen that the samples prepared utilizing the optimized method were more sensitive than before. Which could be observed when comparing the values of dots/µm going from below 0.2 for treated samples (Figure 4.5) to over 0.3 (Figure 4.6). There was still some variations in the biological replicates such as the untreated samples varying in damage level, that will need to be addressed in further studies. As previously mentioned, Zirkin et al. were able to show that the method was sensitive, as they observed more DNA damage when increasing the concentration of H_2O_2 [1]. This could, in this project, only be observed for one biological replicate (Figure 4.7), suggesting that more optimization may be needed for a sensitive method with reproducible results. However, this could not be explored further, due to time limitation and will be addressed in future work.

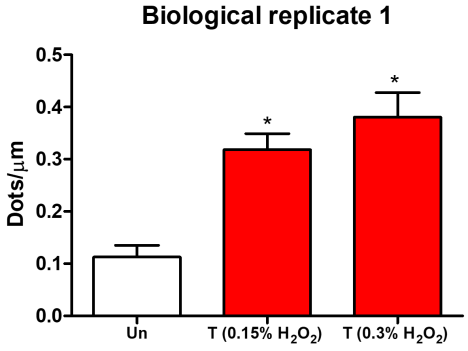

Figure 4.7: DNA damage as dots/µm for untreated (white bars) samples and for samples treated (red bars) with 0.15% and 0.3% H_2O_2 for a duration of 10 minutes. All samples were labeled with the enzyme mix.

As it was observed in the microscopy images that the treated samples were much shorter than the untreated, it was also of interest to investigate the length of the DNA molecules, Figure 4.8. If there was an impact on the length, it could be attributed to direct DNA damage resulting in double-strand breaks (DSBs), which

is not detectable using the enzyme mix specific for ssDNA damage. Alternatively, it is possible that if BER repair is initiated simultaneously on two damaged sites in close proximity on opposite strands, the intermediate in which the damaged base is removed could result in a DSBs [42].

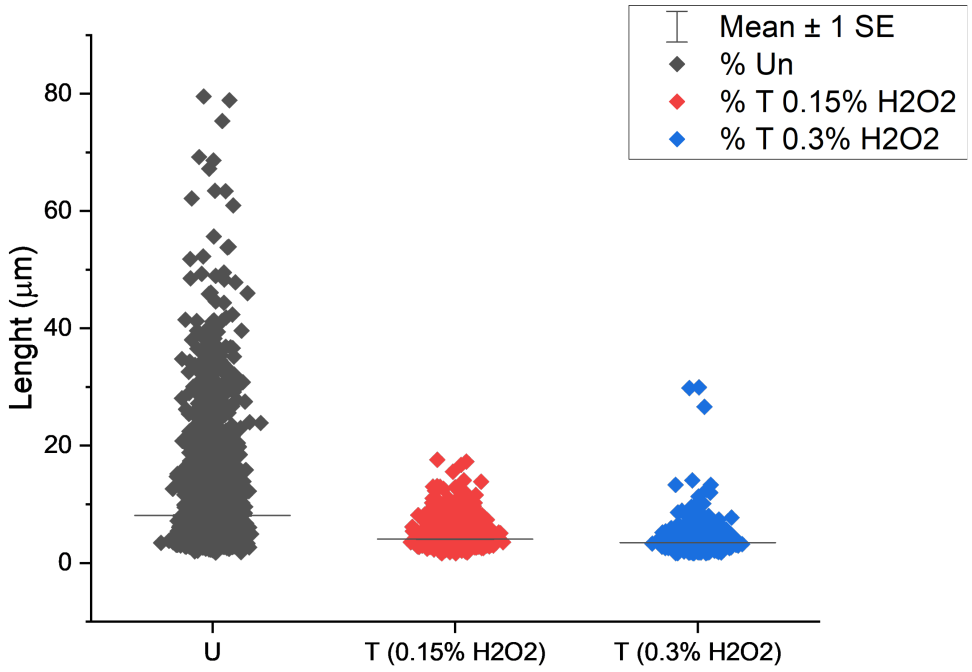

Figure 4.8: Difference in length for untreated, samples treated with 0.15% H_2O_2, and samples treated with 0.3% H_2O_2. visualized with a scatter plot.

The untreated samples generally contained longer DNA strands, while the ones treated with H_2O_2 were more fragmented. There was also a difference between the treated samples, in regard to the concentration added. It seemed that with an increasing concentration, the DNA became more fragmented. Because this was observed for all replicates, it is not likely that the damage was due to the DNA breaking during pipetting, or similarly. The length differences were in addition visualized in the images obtained from the fluorescence microscopy, Figure 4.9. This discovery suggested that length comparison could be used as a complement to µm/dots, to investigate if DSB are formed. To investigate if the fragmentation was due to damage in which DSB are formed directly or due to multiple ssDNA damage sites close to each other, more experiments with decreasing concentration of H_2O_2 could be employed.

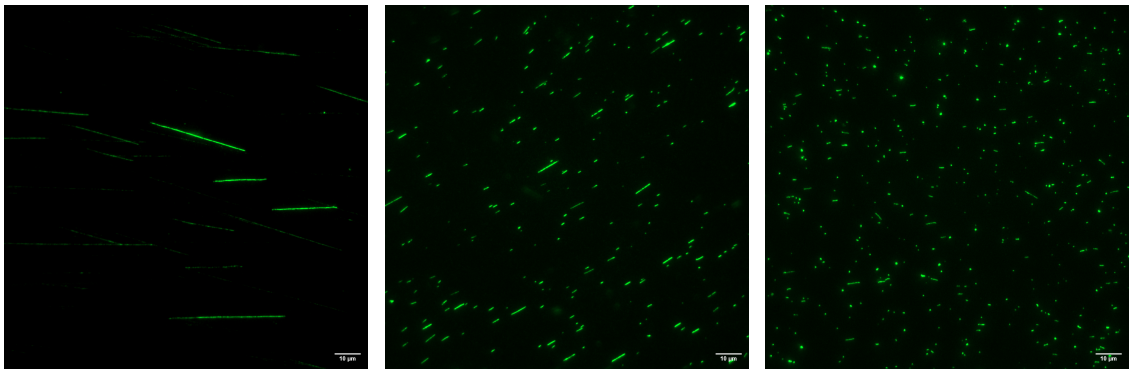

(a) Untreated.

(b) Treated 0.15% H_2O_2, 10 minutes.

(c) Treated 0.3% H_2O_2, 10 minutes.

Figure 4.9: Images portraying the differences in length between untreated sample (4.9a), sample treated with 0.15% H_2O_2 (4.9b), and sample treated with 0.3% H_2O_2 (4.9c). The images are shown in the YOYO-1 channel.

4.3 Antibiotic Experiments

Since the proof-of-concept works, meaning that the SMI method works, it was of interest to conduct experiments using antibiotics as the bacterial stressors.

Some experiments using the SMI method were performed with antibiotics before the final optimization, the conditions and experiments are described in Appendix C.1. The concentrations used were based on Minimum Inhibitory Concentration (MIC) experiments and Growth Curves (GC), data obtained from colleagues work in the Wenzel group, an example shown in Appendix D.1 and D.2. However, since they were performed in the initial stages, the results can not be taken into consideration.

BCP is another fluorescence microscopy method and can be used as a first step to give an indication if there is any effect on the bacterial DNA exposed to a specific compound, before moving on to the SMI method. BCP is faster and has higher throughput compared to the SMI method, meaning that it can be used to check whether the concentrations and treatment times give sufficient effect before moving on to the more laborious and time-consuming SMI method. Alternatively, it can be used as a complement to the SMI method. The SOS response is known to activate genes that are part of the NER pathway to repair damage, while the SMI method utilizes enzymes part of the BER pathway. Meaning that even though there is a strong reaction seen in BCP, it may not correspond to the same in the SMI method and vice versa.

BCP enables the visualization of different components of bacteria using specific dyes. In this study, we utilized DAPI to visualize DNA and Nile red to visualize the cell membrane. Additionally, a *B. subtilis* strain, called UG10, expressing a RecA-GFP fusion protein was employed to observe the localization of RecA-GFP upon antibiotic stress conditions. When there is DNA damage, ssDNA is formed to which RecA can bind turn into its active form [16]. It causes LexA to self-cleave and derepress

genes that can address the damage. RecA-GFP will make a foci, in a location which is assumed to be the spot of the DNA damage, meaning that in a normal cell the protein is cytosolic and in a stressed cell it is in a specific foci. To quantify the results, the percentage of cells containing RecA-GFP foci was measured, Table 4.2.

Table 4.2: Summary of the percentage of cells with RecA-GFP foci for all treatments at 10 and 30 minutes.

Time	Treatment	Percent (%) affected
10 min	Untreated	17
	H_2O_2	70
	Mitomycin C	94
	Ciprofloxacin	97
	Nitrofurantoin	94
	Tetracycline	14
	Trimethoprim	86
30 min	Untreated	15
	H_2O_2	77
	Mitomycin C	99
	Ciprofloxacin	98
	Nitrofurantoin	94
	Tetracycline	33
	Trimethoprim	91

For all treatments, cells were incubated for both 10 and 30 minutes. In general, all except tetracycline showed RecA-GFP foci. The results are discussed in more detail in the following sections.

4.3.1 H_2O_2

H_2O_2 was used at the concentration of 0.3%, Figure 4.10. The compound is a ROS, meaning that it causes oxidative stress and thereby damage the DNA.

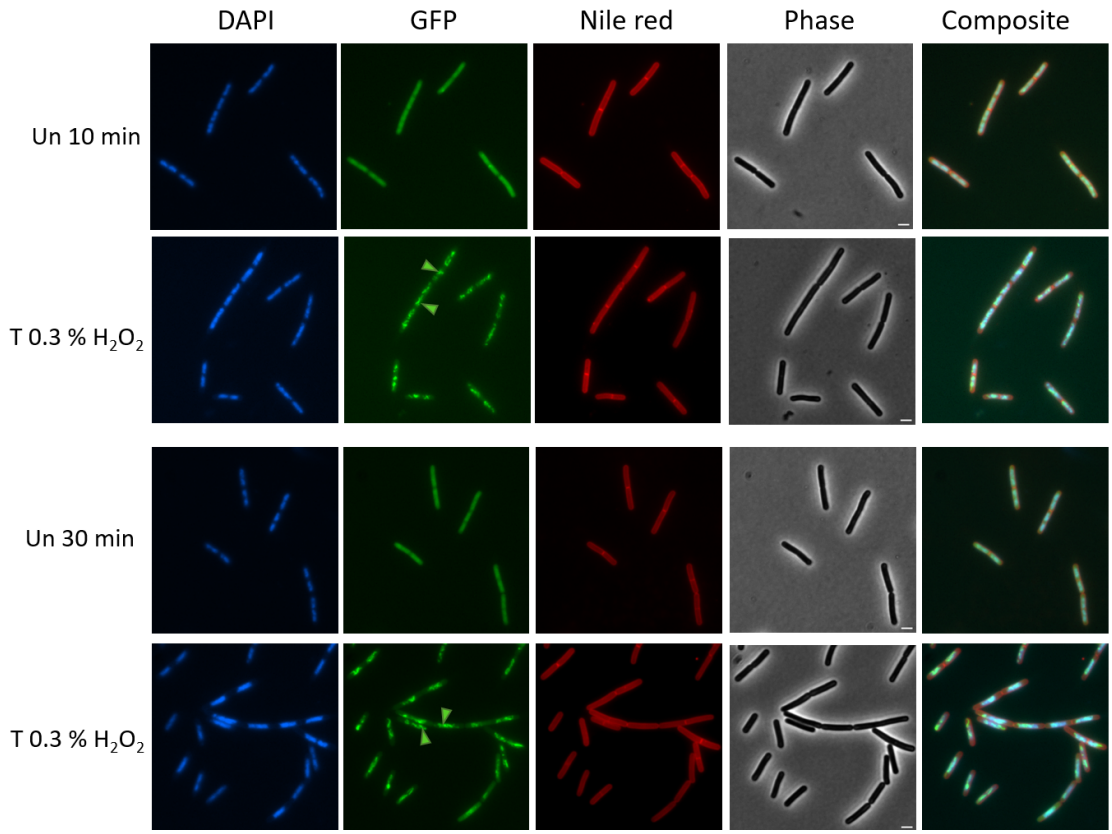

Figure 4.10: BCP of *B. subtilis* UG10 (RecA-GFP) treated with 0.3% H_2O_2 for 10 and 30 minutes, visualized in four different channels DAPI, GFP, Nile red, and phase contrast. Composite is a combination of DAPI, GFP, and Nile red channels. The small arrows indicate RecA-GFP foci.

The treated bacteria contained many foci, examples indicated by arrows, compared to the untreated at both time points. This was also seen in Table 4.2, in which approximately 70% bacterial cells contained RecA-GFP foci. It has previously been shown that H_2O_2 can induce SOS response, specifically oxidative damage by measuring 8-oxoguanine levels [10], also known to be repaired in the BER pathway [7].

4.3.2 Mitomycin C

Mitomycin C with the concentration 0.1 µg/mL was used (Figure 4.11). Mitomycin C is an antibiotic used as a chemotherapy drug. The main purpose is to slow down the growth of cancer cells by targeting DNA synthesis.

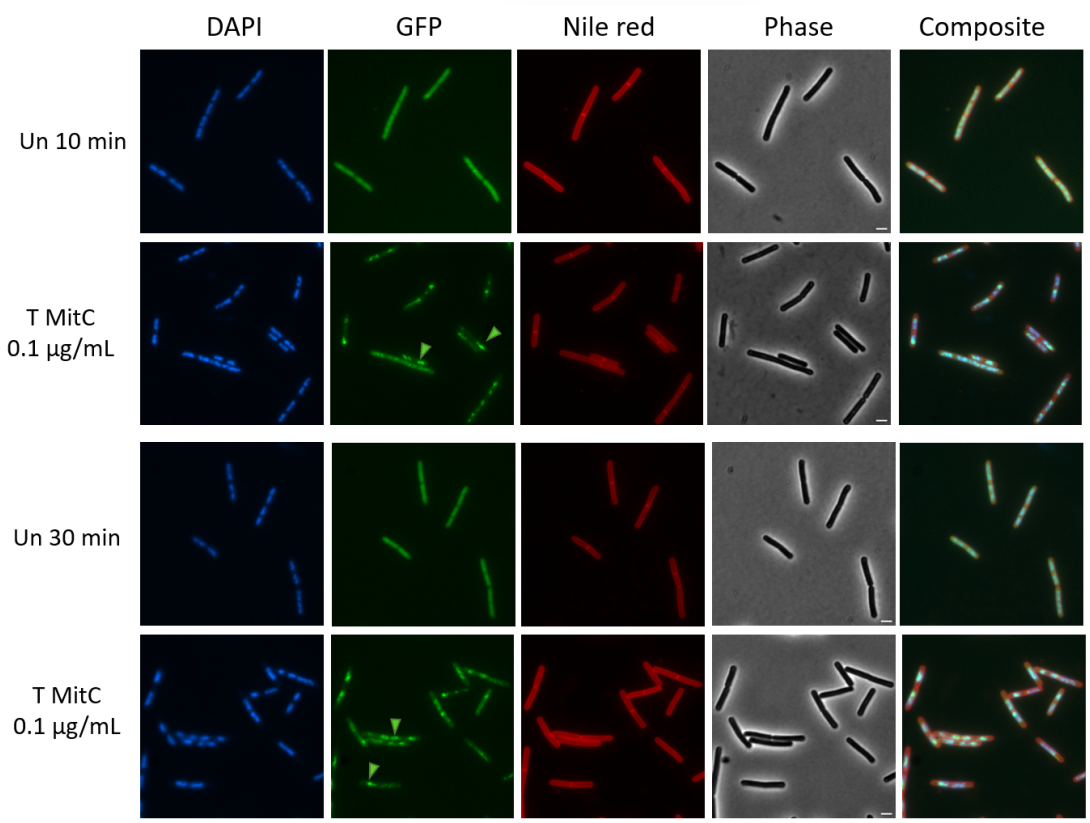

Figure 4.11: BCP of *B. subtilis* UG10 (RecA-GFP) treated with 0.1 µg/mL for 10 and 30 minutes, visualized in four different channels DAPI, GFP, Nile red, and phase contrast. Composite is a combination of DAPI, GFP, and Nile red channels. The small arrows indicate RecA-GFP foci..

In almost all bacterial cells foci can be observed, also seen in Table 4.2. The results were in consensus with previous research. Mitomycin C is known to induce crosslinks between complementary strands of the DNA, hindering DNA replication and transcription. It is thought that the repair of the crosslinks can be achieved through pathways such as NER and homologous recombination [43]. Pathways that can be activated by the SOS response. In addition, it has been shown that RecA production is increased when Mitomycin C is added to bacterial cells, further confirming the obtained results [44].

4.3.3 Ciprofloxacin

Ciprofloxacin (cipro) is known to target the DNA gyrase and topoisomerase IV [24]. The bacterial cells were treated with 1 µg/mL, Figure 4.12.

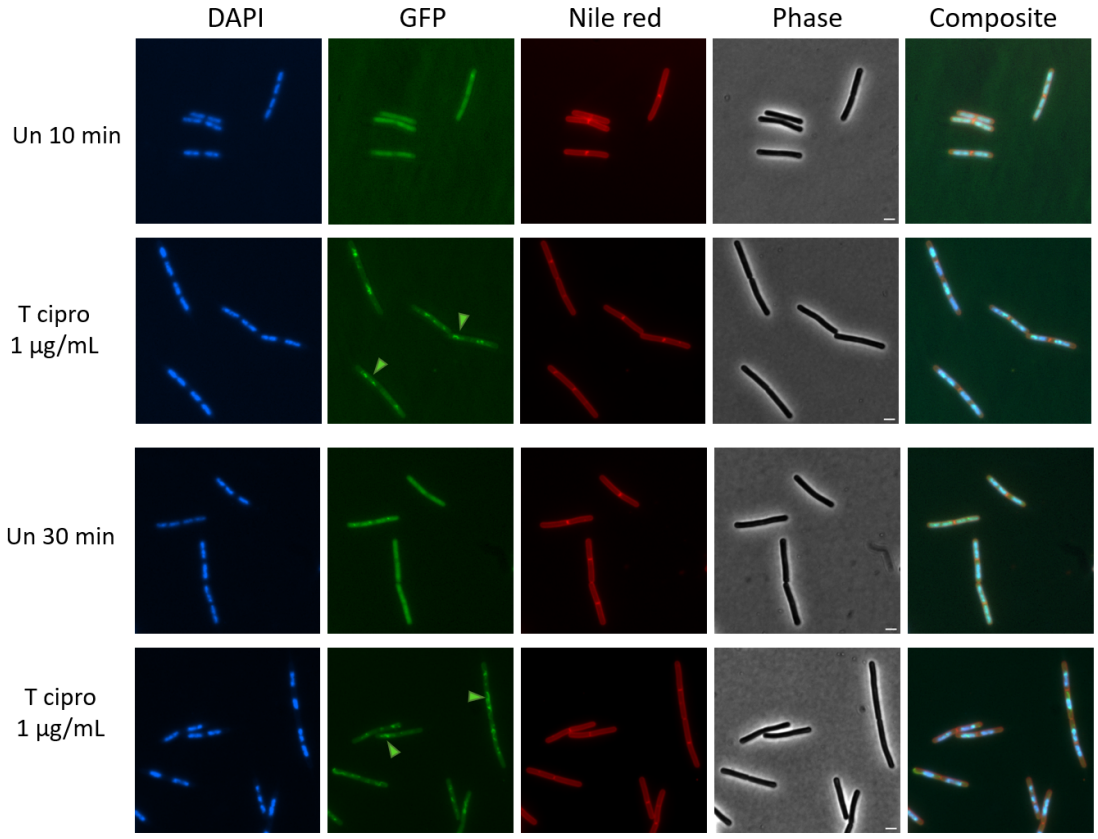

Figure 4.12: BCP of *B. subtilis* UG10 (RecA-GFP) treated with 1 µg/mL ciprofloxacin for 10 and 30 minutes, visualized in four different channels DAPI, GFP, Nile red, and phase contrast. Composite is a combination of DAPI, GFP, and Nile red channels. The small arrows indicate RecA-GFP foci.

As seen both in Figure 4.12 and Table 4.2, most cells contained RecA-GFP foci. As mentioned, cipro binds to DNA gyrase and topoisomerase IV , thus inhibiting the DNA synthesis as well as creating DSB [24]. DSBs can be repaired by the induction of the SOS-response [24].

4.3.4 Nitrofurantoin

Nitrofurantoin (NFT) is an antibiotic that targets the cellular macromolecules. It was tested with the concentration of 25 µM, Figure 4.13.

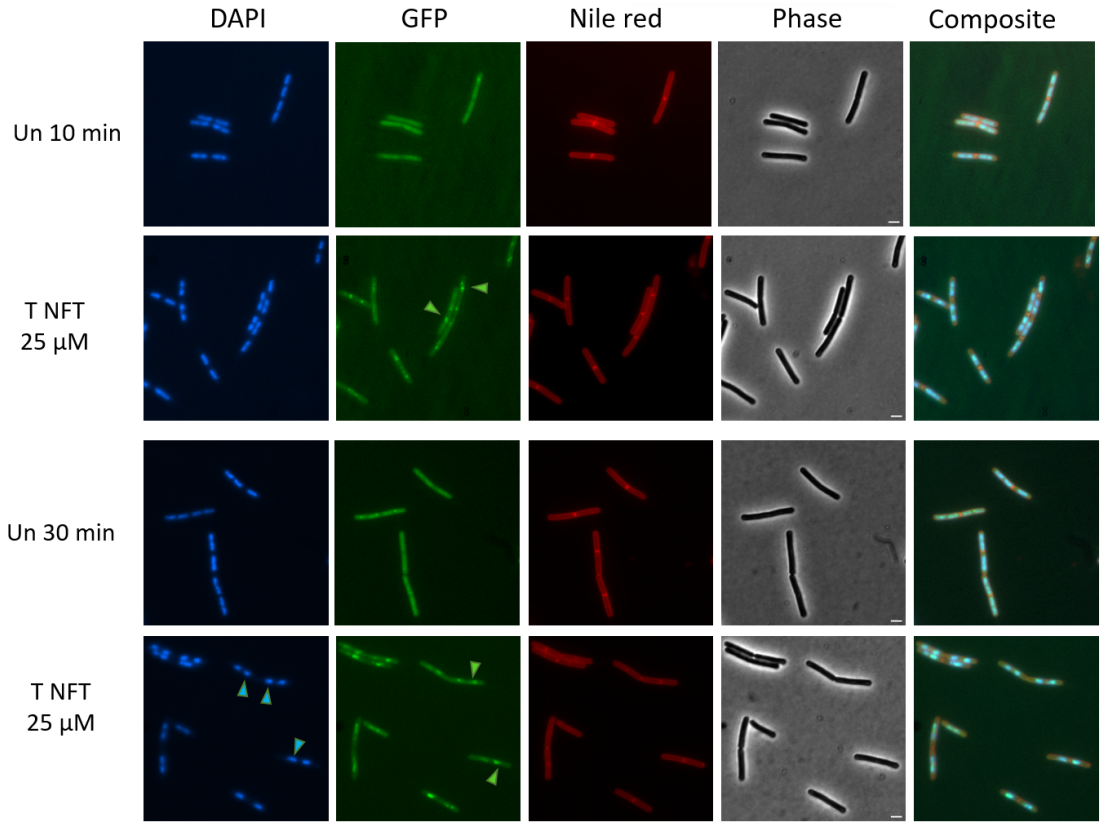

Figure 4.13: BCP of *B. subtilis* UG10 (RecA-GFP) treated with 25 µM nitrofurantoin for 10 and 30 minutes, visualized in four different channels DAPI, GFP, Nile red, and phase contrast. Composite is a combination of DAPI, GFP, and Nile red channels. The small arrows in the GFP channel indicate RecA-GFP fociand the arrows in the DAPI channel indicate nucleic compaction.

Most bacterial cells contained RecA-GFP foci, both for 10 and 30 minutes of incubation (Figure 4.13, Table 4.2). It has been proposed that the activation of NFT induces an unkown reactive species, likely nitrogen that can result in damage to DNA, proteins and lipids [23]. As mentioned before the SOS response can be activated upon oxidative DNA damage. Looking at the DAPI channel images, especially after 30 minutes incubation, nucleic compaction was observed, as indicated with the blue arrows. Although, the results would have to be confirmed through data analysis, by quantitatively measuring the compaction. However, due to time limitation, this analysis was not performed.

4.3.5 Tetracycline

Tetracycline (tet) is an antibiotic that targets the protein synthesis by preventing aminoacyl-tRNA from attaching to the ribosomal acceptor site. It was tested with the concentration 2.5 µg/mL, Figure 4.14.

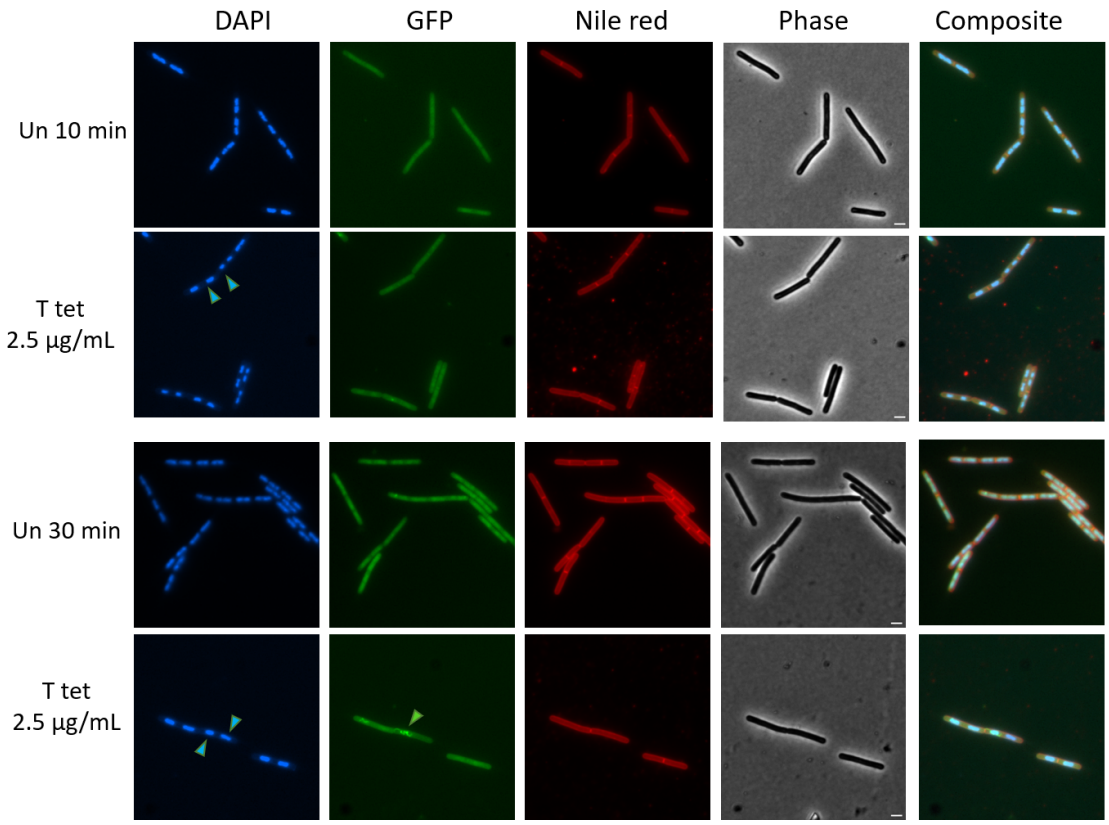

Figure 4.14: BCP of *B. subtilis* UG10 (RecA-GFP) treated with 2.5 µg/mL for 10 and 30 minutes, visualized in four different channels DAPI, GFP, Nile red, and phase contrast. Composite is a combination of DAPI, GFP, and Nile red channels. The small arrows in the GFP channel indicate RecA-GFP foci, while the arrows in the DAPI channel indicate nucleic compaction.

Analyzing the bacterial cells treated with tet, there were few cells containing RecA-GFP foci (Figure 4.14, Table 4.2). At 10 minutes, there was no observed difference compared to the untreated samples and at 30 minutes there was a slight difference. However, not enough data to conclude that there was an increase in RecA-GFP foci. Looking at the DAPI channel microscopy images, there was an indication that the nucleoid was more compacted compared to the untreated bacteria, suggesting that there was some other influence in DNA unrelated to RecA.

4.3.6 Trimethoprim

Trimethoprim (trim) targets the folic acid pathway. The compound was added with the concentration 8 µg/mL, Figure 4.15.

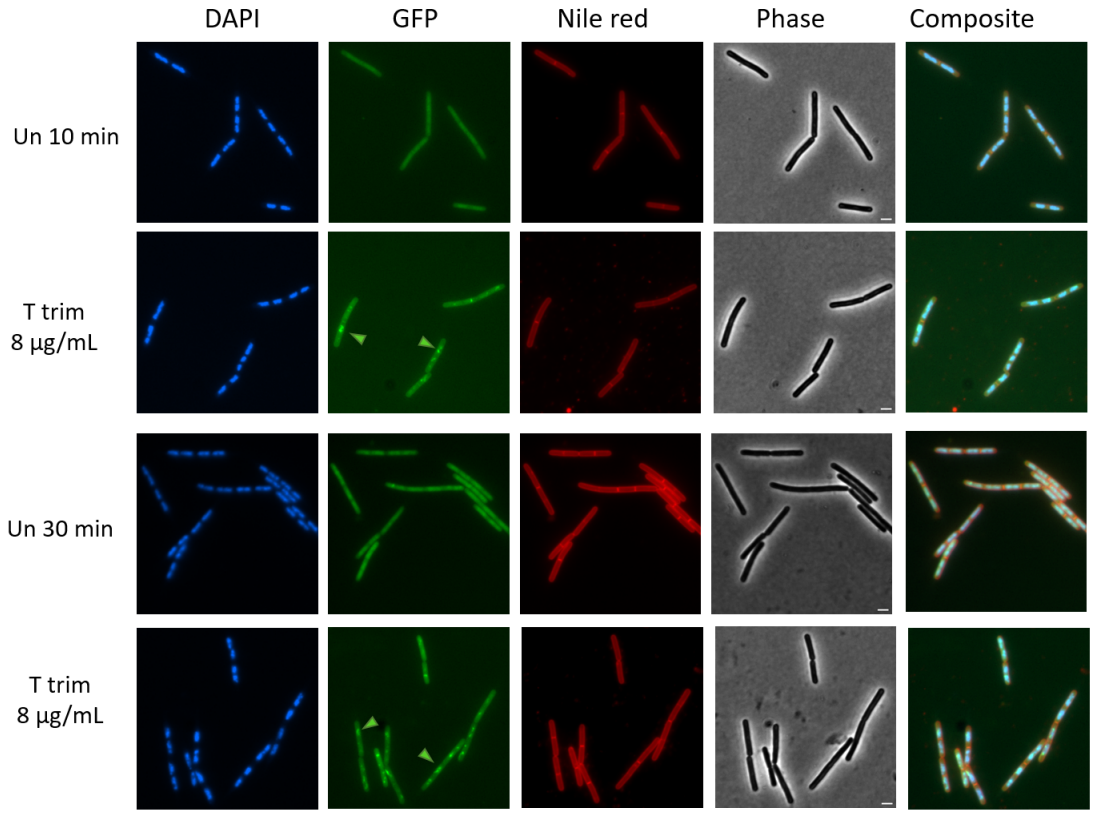

Figure 4.15: BCP of *B. subtilis* UG10 (RecA-GFP) treated with 8 µg/mL for 10 and 30 minutes, visualized in four different channels DAPI, GFP, Nile red, and phase contrast. Composite is a combination of DAPI, GFP, and Nile red channels. The small arrows indicate RecA-GFP foci.

In general, most cells contained RecA-GFP foci (Figure 4.15, Figure 4.2). Trim exerts its effects by inhibiting the enzyme dihydrofolate reductase, thereby blocking the conversion of dihydrofolate to tetrahydrofolate [26]. This inhibition disrupts the production of tetrahydrofolate, which subsequently impacts DNA replication and protein synthesis processes. In previous studies it was determined that the SOS response is induced in presence of trim [45], supporting the obtained result. It was also reported that trim increases the formation of ROS, creating DSBs in the DNA.

4.4 Outlook

To continue the work presented in the thesis, the first step is to ensure reproducibility of the method, so that the results obtained are statistically reliable and can be confidently compared and validated. This includes conducting more biological replicates, carefully documenting any changes in the execution as well as potential factors that may contribute to the observed variation.

After establishing the method, the next step would be employ antibiotics to investigate DNA damage. Both by using the enzyme mix, as well as employing the method in which individual enzymes are added to establish the prominent type(s) of damage

induced.

The experiments in this thesis were performed *in vivo*, as the bacterial stressor compound was added to the live cell. This means that DNA damage can be caused either direct; by directly targeting the DNA, or indirect; by targeting something else that indirectly affects the DNA. Thus, it is interesting to also perform *ex vivo* experiments, in which the DNA is isolated prior addition of a stressor compound. These experiments have been started by Aysha Arshad in the Wenzel group at Chalmers University of Technology.

It would also be interesting to investigate and employ the method for different model organisms, such as Gram-negative bacteria. Gram-positive and negative bacteria do not share the same cell envelope, as Gram-negative bacteria contains two lipid membranes (outer and inner membranes) compared to one.

5
Conclusion

A fluorescence microscopy based single molecule imaging (SMI) method was developed to detect DNA damage in bacteria. This method enables future application in detecting antibiotic induced DNA damage. During the optimization, several factors were observed to play a crucial role. These factors; purity of chemicals and DNA quantity, are important for DNA quality and also for detection of DNA damage. Moreover, it was observed that the act of repeatedly temperature shocking *B.subtilis* potentially cause DNA damage in bacteria, thus single-use bacterial aliquots were utilized to mitigate the issue. In conclusion, the developed method worked well by showing the DNA damage in dots/µm and length. In the future, extended experiments to more thoroughly assess the reproducibility and robustness of the method also in the single enzyme assay and antibiotic experiments will be performed.

Bibliography

[1] Zirkin S, Fishman S, Sharim H, Michaeli Y, Don J, Ebenstein Y. Lighting up individual DNA damage sites by in vitro repair synthesis. Journal of the American Chemical Society. 2014;136(21):7771-6.

[2] Maslowska KH, Makiela-Dzbenska K, Fijalkowska IJ. The SOS system: a complex and tightly regulated response to DNA damage. Environmental and molecular mutagenesis. 2019;60(4):368-84.

[3] Munita JM, Arias CA. Mechanisms of antibiotic resistance. Microbiology spectrum. 2016;4(2):4-2.

[4] World Health Organization. Antimicrobial resistance; 2021. Available from: `https://www.who.int/en/news-room/fact-sheets/detail/antimicrobial-resistance`.

[5] Singer AC, Shaw H, Rhodes V, Hart A. Review of antimicrobial resistance in the environment and its relevance to environmental regulators. Frontiers in microbiology. 2016;7:1728.

[6] Reygaert WC. An overview of the antimicrobial resistance mechanisms of bacteria. AIMS microbiology. 2018;4(3):482.

[7] Wozniak KJ, Simmons LA. Bacterial DNA excision repair pathways. Nature Reviews Microbiology. 2022:1-13.

[8] Solanky D, Haydel SE. Adaptation of the neutral bacterial comet assay to assess antimicrobial-mediated DNA double-strand breaks in Escherichia coli. Journal of microbiological methods. 2012;91(2):257-61.

[9] Clarke RS, Ha KP, Edwards AM. Multiple classes of bactericidal antibiotics cause DNA double strand breaks in Staphylococcus aureus. bioRxiv. 2021:2021-03.

[10] Kim H, Lee DG. Contribution of SOS genes to H2O2-induced apoptosis-like death in Escherichia coli. Current Genetics. 2021;67(6):969-80.

[11] Singh V, Johansson P, Ekedahl E, Lin YL, Hammarsten O, Westerlund F. Quantification of single-strand DNA lesions caused by the topoisomerase II poison etoposide using single DNA molecule imaging. Biochemical and Biophysical Research Communications. 2022;594:57-62.

[12] Singh V, Johansson P, Lin YL, Hammarsten O, Westerlund F. Shining light on single-strand lesions caused by the chemotherapy drug bleomycin. DNA repair. 2021;105:103153.

[13] Errington J, van der Aart LT. Microbe profile: Bacillus subtilis: model organism for cellular development, and industrial workhorse. Microbiology. 2020;166(5):425.

[14] Baron S. Medical microbiology. 1996.

[15] McQuaid KT, Pipier A, Cardin CJ, Monchaud D. Interactions of small molecules with DNA junctions. Nucleic Acids Research. 2022;50(22):12636-56.

[16] Lenhart JS, Schroeder JW, Walsh BW, Simmons LA. DNA repair and genome maintenance in Bacillus subtilis. Microbiology and molecular biology reviews. 2012;76(3):530-64.

[17] Podlesek Z, Žgur Bertok D. The DNA damage inducible SOS response is a key player in the generation of bacterial persister cells and population wide tolerance. Frontiers in microbiology. 2020;11:1785.

[18] Gao B, Liang L, Su L, Wen A, Zhou C, Feng Y. Structural basis for regulation of SOS response in bacteria. Proceedings of the National Academy of Sciences. 2023;120(2):e2217493120.

[19] McNeill DR, Whitaker AM, Stark WJ, Illuzzi JL, McKinnon PJ, Freudenthal BD, et al. Functions of the major abasic endonuclease (APE1) in cell viability and genotoxin resistance. Mutagenesis. 2020;35(1):27-38.

[20] Chang IY, Kim JN, Maeng YH, Yoon SP. Apurinic/apyrimidinic endonuclease 1, the sensitive marker for DNA deterioration in dextran sulfate sodium-induced acute colitis. Redox Report. 2013;18(5):165-73.

[21] Sarre A, Stelter M, Rollo F, De Bonis S, Seck A, Hognon C, et al. The three Endonuclease III variants of Deinococcus radiodurans possess distinct and complementary DNA repair activities. DNA repair. 2019;78:45-59.

[22] Huttner A, Verhaegh EM, Harbarth S, Muller AE, Theuretzbacher U, Mouton JW. Nitrofurantoin revisited: a systematic review and meta-analysis of controlled trials. Journal of Antimicrobial Chemotherapy. 2015;70(9):2456-64.

[23] Wenzel M. Do we really understand how antibiotics work?. Future Medicine; 2020.

[24] Ojkic N, Lilja E, Direito S, Dawson A, Allen RJ, Waclaw B. A roadblock-and-kill mechanism of action model for the DNA-targeting antibiotic ciprofloxacin. Antimicrobial agents and chemotherapy. 2020;64(9):e02487-19.

[25] Chopra I, Roberts M. Tetracycline antibiotics: mode of action, applications, molecular biology, and epidemiology of bacterial resistance. Microbiology and molecular biology reviews. 2001;65(2):232-60.

[26] Giroux X, Su WL, Bredeche MF, Matic I. Maladaptive DNA repair is the ultimate contributor to the death of trimethoprim-treated cells under aerobic and anaerobic conditions. Proceedings of the National Academy of Sciences. 2017;114(43):11512-7.

[27] Tomasz M. Mitomycin C: small, fast and deadly (but very selective). Chemistry & biology. 1995;2(9):575-9.

[28] Trastoy MO, Defais M, Larminat F. Resistance to the antibiotic Zeocin by stable expression of the Sh ble gene does not fully suppress Zeocin-induced DNA cleavage in human cells. Mutagenesis. 2005;20(2):111-4.

[29] Waring M, Wakelin L. Echinomycin: a bifunctional intercalating antibiotic. Nature. 1974;252(5485):653-7.

[30] May LG, Madine MA, Waring MJ. Echinomycin inhibits chromosomal DNA replication and embryonic development in vertebrates. Nucleic acids research. 2004;32(1):65-72.

[31] Nonejuie P, Burkart M, Pogliano K, Pogliano J. Bacterial cytological profiling rapidly identifies the cellular pathways targeted by antibacterial molecules. Proceedings of the National Academy of Sciences. 2013;110(40):16169-74.
[32] Schäfer AB, Wenzel M. A how-to guide for mode of action analysis of antimicrobial peptides. Frontiers in cellular and infection microbiology. 2020;10:540898.
[33] Kaur G, Lewis JS, van Oijen AM. Shining a spotlight on DNA: single-molecule methods to visualise DNA. Molecules. 2019;24(3):491.
[34] Goyal G, Ekedahl E, Nyblom M, Krog J, Fröbrant E, Brander M, et al. A simple cut and stretch assay to detect antimicrobial resistance genes on bacterial plasmids by single-molecule fluorescence microscopy. Scientific Reports. 2022;12(1):9301.
[35] Spizizen J. Transformation of biochemically deficient strains of Bacillus subtilis by deoxyribonucleate. Proceedings of the National Academy of Sciences. 1958;44(10):1072-8.
[36] Saeloh D, Tipmanee V, Jim KK, Dekker MP, Bitter W, Voravuthikunchai SP, et al. The novel antibiotic rhodomyrtone traps membrane proteins in vesicles with increased fluidity. PLoS pathogens. 2018;14(2):e1006876.
[37] Koo BM, Kritikos G, Farelli JD, Todor H, Tong K, Kimsey H, et al. Construction and analysis of two genome-scale deletion libraries for Bacillus subtilis. Cell systems. 2017;4(3):291-305.
[38] Gray D, Wang B, Gamba P, Strahl H, Hamoen L. Membrane depolarization kills dormant Bacillus subtilis cells by generating a lethal dose of ROS. 2021.
[39] Green MR, Sambrook J. Isolation of high-molecular-weight DNA using organic solvents. Cold Spring Harbor Protocols. 2017;2017(4):pdb-prot093450.
[40] Rueden CT, Schindelin J, Hiner MC, DeZonia BE, Walter AE, Arena ET, et al. ImageJ2: ImageJ for the next generation of scientific image data. BMC bioinformatics. 2017;18:1-26.
[41] Simbolo M, Gottardi M, Corbo V, Fassan M, Mafficini A, Malpeli G, et al. DNA qualification workflow for next generation sequencing of histopathological samples. PloS one. 2013;8(6):e62692.
[42] Cannan WJ, Pederson DS. Mechanisms and consequences of double-strand DNA break formation in chromatin. Journal of cellular physiology. 2016;231(1):3-14.
[43] Lee YJ, Park SJ, Ciccone SL, Kim CR, Lee SH. An in vivo analysis of MMC-induced DNA damage and its repair. Carcinogenesis. 2006;27(3):446-53.
[44] Giacomoni PU. Induction by mitomycin C of recA protein synthesis in bacteria and spheroplasts. Journal of Biological Chemistry. 1982;257(24):14932-6.
[45] Sangurdekar DP, Zhang Z, Khodursky AB. The association of DNA damage response and nucleotide level modulation with the antibacterial mechanism of the anti-folate drug trimethoprim. BMC genomics. 2011;12:1-14.

A

Appendix A

A.1 Protocol: Preparation of 168CA aliquots

The following protocol describes the method to make single-use aliquots of *B. subtilis* 168CA that was used for chromosomal DNA isolation.

1. Inoculate *B. subtilis* 168CA cells in 2 mL LB in 50 mL Eppendorf tubes and incubate at 37℃ and 200 rpm for a maximum of 16 h.
2. In the morning: dilute cells 1:100 in 20 mL LB in an Erlenmeyer flask and grow until an OD_{600} of 0.5 in 37℃ and 200 rpm.
3. Add 13.3 mL sterile 50% glycerol to the Erlenmeyer flask in a ratio of 1.5 cells:1 glycerol.
4. Move 2 mL of the mixture to 2 mL Eppendorf tubes and store in -80℃.
5. To use: add one aliquot to an Erlenmeyer flask with 20 mL LB and incubate.

A.2 Protocol: Chromosomal DNA isolation

1. Centrifuge samples at 7830 rpm for 5 minutes.
2. Wash the pellet in 500 μL TES buffer and move the cells to 2 mL Eppendorf tubes and centrifuge at 14000 rpm for 1 minute.
3. Resuspend the pellet in 750 μL TES buffer. Add 25 μL Lysozyme (20 mg/mL) and 25 μL RNase (10 mg/mL) and incubate on a heat block at 37° and 740 rpm for 30 minutes.
4. Add 25 μL Pronase (10 mg/mL) and 30 μL Sarkosyl (30%) and mix by inverting the tubes. Incubate on a heat block at 37° and 740 rpm for 60 minutes.

   Perform step 5 to 7 under the fumehood with gloves.

5. Add 250 μL equilibrated phenol and 250 μL chloroform. Mix by inverting the tubes for 2 minutes and centrifuge at 14000 rpm for 4 minutes.
6. Take 700 μL of the upper layer with a cut pipette tip and add to a new 2 mL Eppendorf tube with 500 μL chloroform. Mix by inverting the tubes for 2 minutes and centrifuge at 14000 rpm for 4 minutes.
7. Take 500 μL of the upper layer with a cut pipette tip and add to a new 1.5 mL Eppendorf tube with 1 mL isopropanol. Mix by inverting the tubes until a white "cloud" of DNA can be seen in the mixture. Centrifuge at 14000 rpm for 15 minutes.
8. Discard the supernatant and add 500 μL 70% ethanol. Mix by inverting the tubes for 2 minutes.

9. Repeat step 8.
10. Remove the ethanol with a pipette and put the Eppendorf tubes upside down for the remaining ethanol to evaporate.
11. Solubilize the DNA by adding 100 μL milli-Q water.

B

Appendix B

B.1 MATLAB settings

The script that was used to quantify the damage on the bacterial DNA was developed in Tobias Ambjörnsson's research group at Lund University. Below follows the settings that were used (Figure B.1).

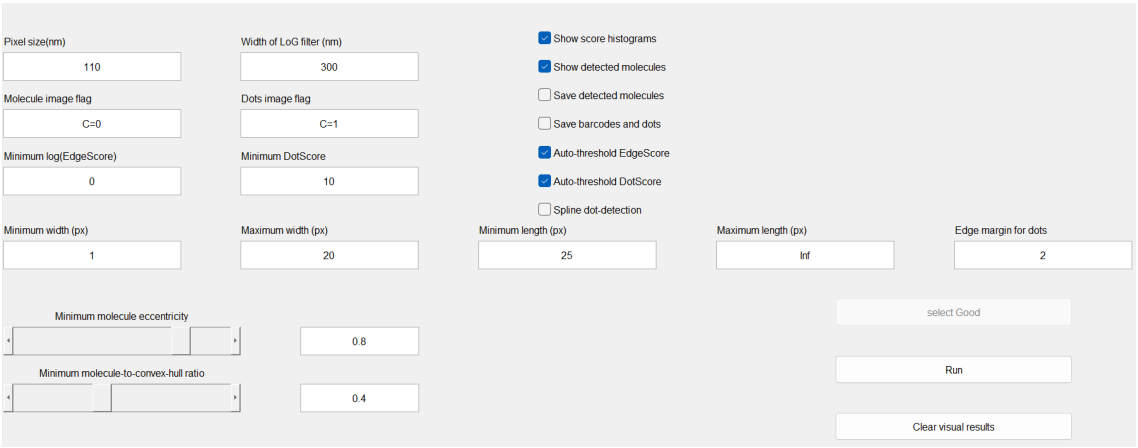

Figure B.1: The setting that were used on the MATLAB script to quantify DNA damage.

Pixel size was chosen based on the pixel size for the used fluorescence microscope, in this case 110 nm. The maximum width was set to 20, to prevent the program from recognizing non-stretched DNA. The Edge- and Dotscore were set to auto threshold. The minimum length was set to 25, to be able to recognize fragmented DNA. The Edge margin for dots was set to 2 pixels, meaning that dots that were right at the edges of the molecules were not taken into consideration. The minimum molecule eccentricity and the minimum-to-convex-hull ratio were set to 0.8 and 0.4, respectively, to ensure that fully stretched molecules were recognized, but not so strict that long DNA strands with a slight curve were disregarded.

C

Appendix C

C.1 Additional SMI experiments

More experiments than those presented in the result and discussion section of the thesis were performed, Figure C.1. However, they can not be included since the experiments were performed and the results were obtained before the final optimization.

Table C.1: The DNA damage and labeling experiments performed during the project, and in which the results are not reliable as they were performed before the final optimization.

Strain	Treatment	Replicates	Time Point	Enzymes
168CA	UV (365 nm)	4	30 min	Enzyme mix[a] + PDG[b]
2682	UV (365 nm)	1	30 min	Enzyme mix[a] + PDG[b]
BKE16940	UV (365 nm)	1	30 min	Enzyme mix[a] + PDG[b]
168CA	Ciprofloxacin (1 μg/mL)	2	30 min	Enzyme mix[a]
168CA	Ciprofloxacin (2 μg/mL)	3	30 min	Enzyme mix[a]
168CA	Nitrofurantoin (25 μM)	1	10 min	Enzyme mix[a]
168CA	Nitrofurantoin (25 μM)	1	30 min	Enzyme mix[a]
168CA	Tetracycline (2.5 μg/mL)	1	30 min	Enzyme mix[a]
168CA	Mitomycin C (0.1 μg/mL)	3	30 min	Enzyme mix[a]

[a]The enzyme mix consists of the enzymes: APE1, Endo III, Endo IV, Endo VIII, FPG, and UDG.
[b]The enzyme PDG is specific for UV-induced damage as it recognizes and removes CPDs and 6-4 photoproducts.

The experiments with UV were at first intended as a proof-of-concept, however, no significant difference was observed between untreated and treated samples. In addition, the enzyme PDG which is specific for UV-induced damage had to be added, which defeated the purpose to show that the method worked with the chosen enzymes in the enzyme mix (APE1, Endo III, Endo IV, Endo VIII, FPG, UDG).

The experiments with the antibiotics ciprofloxacin, nitrofurantoin and tetracycline were performed during the initial experiments, before final optimization. The experiments with Mitomycin C were performed during the optimization process. However, the enzyme mix was used to label the damage and previous research has shown that a specific enzyme, Endo VII, is needed to recognize the damage caused by Mitomycin C.

D

Appendix D

D.1 Minimum Inhibitory Concentration (MIC): Zeocin and Echinomycin

The Minimum Inhibitory Concentration (MIC) experiments were carried out by Aysha Arshad in the Wenzel group at Chalmers University of Technology. Overnight culture of 168CA *B. subtilis* was diluted 1:100 and grown to an OD_{600} of 1. A 96-microwell plate was used, in which the first column was a sterile control and the last a growth control. In two rows, a two-fold serial dilution was performed with zeocin or echinomycin. $5x10^5$ cells/mL was added to each well and the plate was incubated at 37℃ for 16 hours. The MIC was determined by eye, and is presented in Table D.1

Table D.1: MIC for zeocin and echinomycin.

Antibiotic	MIC (μg/mL)
Zeocin	2.7
Echinomycin	0.125

D.2 Growth Curve (GC): Zeocin and Echinomycin

Growth curve (GC) experiments were carried out by Aysha Arshad in the Wenzel group at Chalmers University of Technology. Overnight culture of 168CA *B.subtilis* was diluted 1:100 and grown until an OD_{600} of 0.3, then the antibiotic of interest was added. The OD_{600} was then measured every 15 minutes until stationary phase was reached. The antibiotics tested were zeocin (Figure D.1a) and echinomycin (Figure D.1b) with concentrations of 0.5X, 1X, 2X, and 4X of the respective MICs (Table D.1).

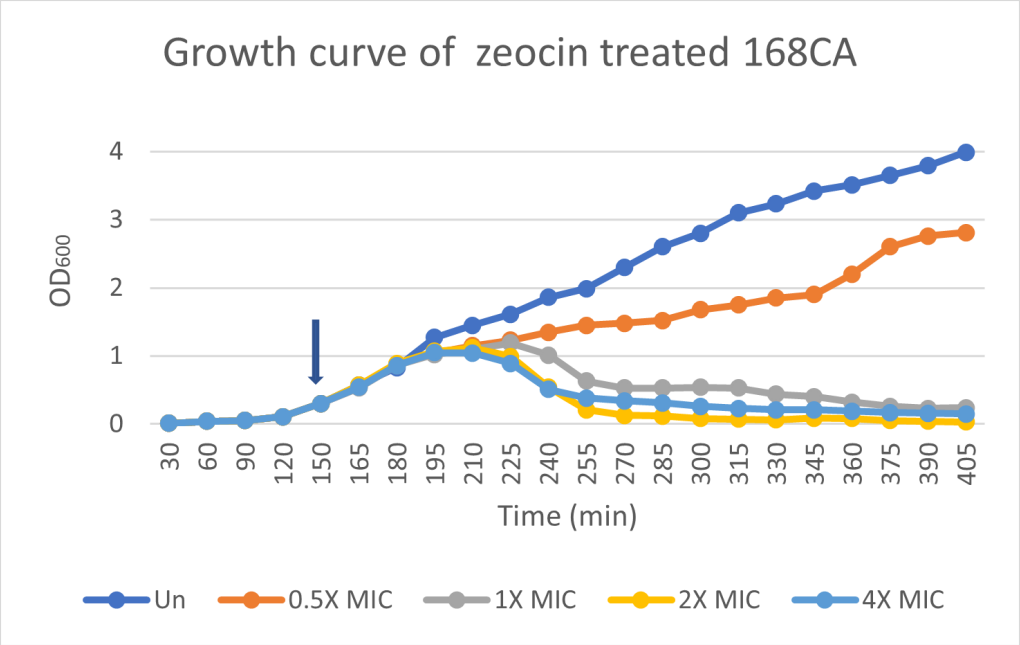

(a) Growth curve for zeocin.

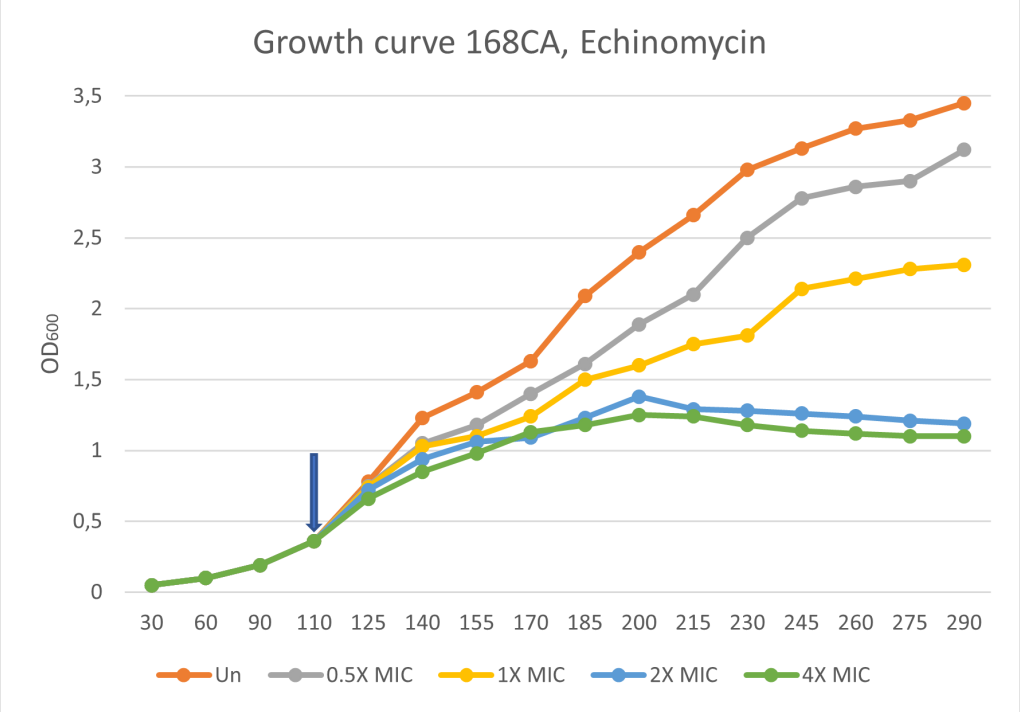

(b) Growth curve for echinomycin.

Figure D.1: Growth curves for zeocin (D.1a) and echinomycin (D.1b), tested with 0.5X, 1X, 2X, and 4X of MIC.

The idea was to obtain a concentration in which the cell growth is inhibited without killing the bacteria. In this case 0.5X MIC for zeocin, corresponding to a concentration of 1.35 µg/mL and 1X MIC for echinomycin, corresponding to a concentration of 0.125 µg/mL.

E

Appendix E

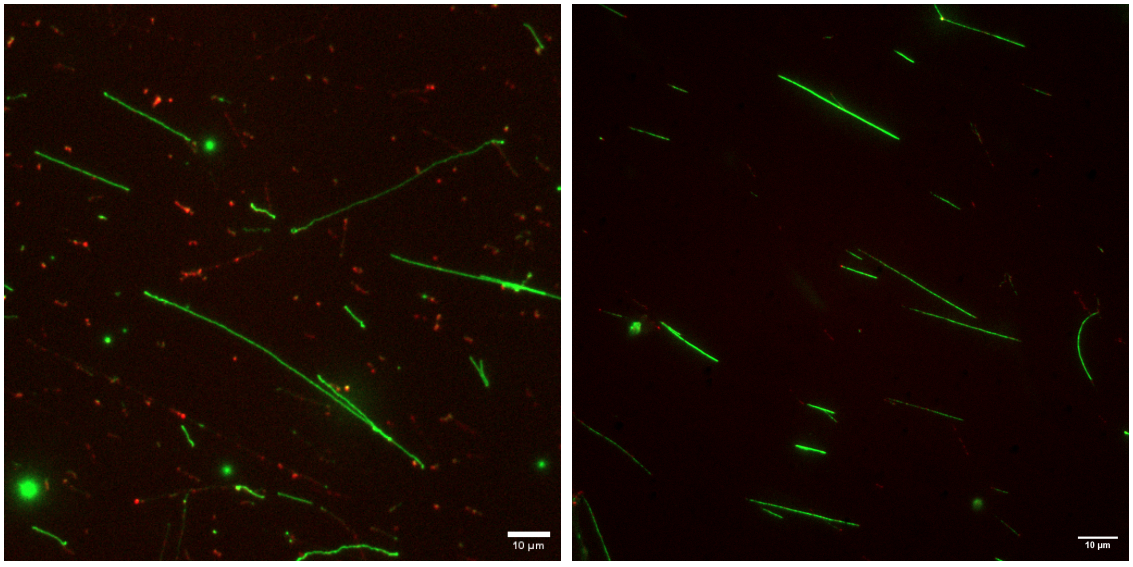

(a) Microscopy image before changing the ethanol

(b) Microscopy image after changing the ethanol

Figure E.1: Microscopy images before (E.1a) and after (E.1b) ethanol change in the DNA isolation process.

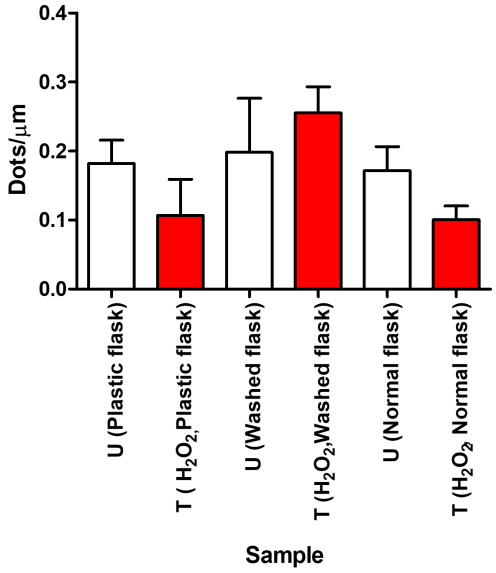

Figure E.2: Comparison between flask with normal wash (washed 1X), flask with special wash (washed 2X), and disposable plastic flask. All labeled with the enzyme mix.

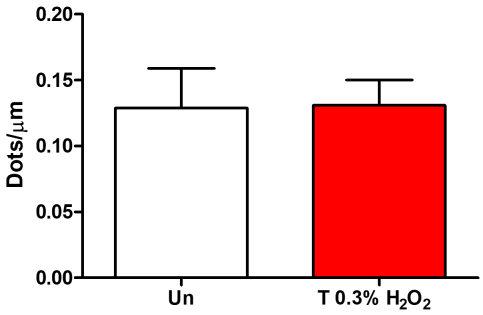

(a) Biological replicate 1

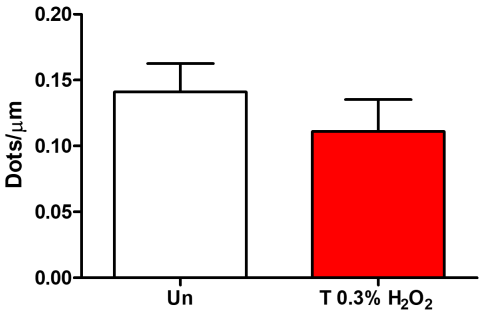

(b) Biological replicate 2

Figure E.3: Untreated and Treated samples with 0.3% H_2O_2 for 30 minutes with a newly prepared stock of 168CA *B. subtilis*.

F

Appendix F

F.1 Box links for data

The data presented in the results and discussion can be accessed using the following Box links for BCP and for the SMI method, in which the experiments are divided into two groups (old method and optimized method).

DEPARTMENT OF LIFE SCIENCES
CHALMERS UNIVERSITY OF TECHNOLOGY
Gothenburg, Sweden
www.chalmers.se

CHALMERS
UNIVERSITY OF TECHNOLOGY